

# Journal Pre-proof

Structure-activity relationship studies and bioactivity evaluation of 1,2,3-triazole containing analogues as a selective sphingosine kinase-2 inhibitors

Vijai Kumar Reddy Tangadanchu, Hao Jiang, Yanbo Yu, Thomas J.A. Graham, Hui Liu, Buck E. Rogers, Robert Gropler, Joel Perlmutter, Zhude Tu



PII: S0223-5234(20)30685-1

DOI: <https://doi.org/10.1016/j.ejmech.2020.112713>

Reference: EJMECH 112713

To appear in: *European Journal of Medicinal Chemistry*

Received Date: 21 April 2020

Revised Date: 10 July 2020

Accepted Date: 29 July 2020

Please cite this article as: V.K. Reddy Tangadanchu, H. Jiang, Y. Yu, T.J.A. Graham, H. Liu, B.E. Rogers, R. Gropler, J. Perlmutter, Z. Tu, Structure-activity relationship studies and bioactivity evaluation of 1,2,3-triazole containing analogues as a selective sphingosine kinase-2 inhibitors, *European Journal of Medicinal Chemistry*, <https://doi.org/10.1016/j.ejmech.2020.112713>.

This is a PDF file of an article that has undergone enhancements after acceptance, such as the addition of a cover page and metadata, and formatting for readability, but it is not yet the definitive version of record. This version will undergo additional copyediting, typesetting and review before it is published in its final form, but we are providing this version to give early visibility of the article. Please note that, during the production process, errors may be discovered which could affect the content, and all legal disclaimers that apply to the journal pertain.

© 2020 Elsevier Masson SAS. All rights reserved.

## Graphical Abstract

### Structure-activity relationship studies and bioactivity evaluation of 1,2,3-triazole containing analogues as a selective sphingosine kinase-2 inhibitors

Vijai Kumar Reddy Tangadanchu <sup>a</sup>, Hao Jiang <sup>a</sup>, Yanbo Yu <sup>a</sup>, Thomas J. A. Graham <sup>b</sup>, Hui Liu <sup>c</sup>,  
Buck E. Rogers <sup>d</sup>, Robert Gropler <sup>a</sup>, Joel Perlmutter <sup>a,e</sup>, Zhude Tu <sup>a,\*</sup>

<sup>a</sup> Department of Radiology, Washington University School of Medicine, St. Louis, Missouri 63110, USA.

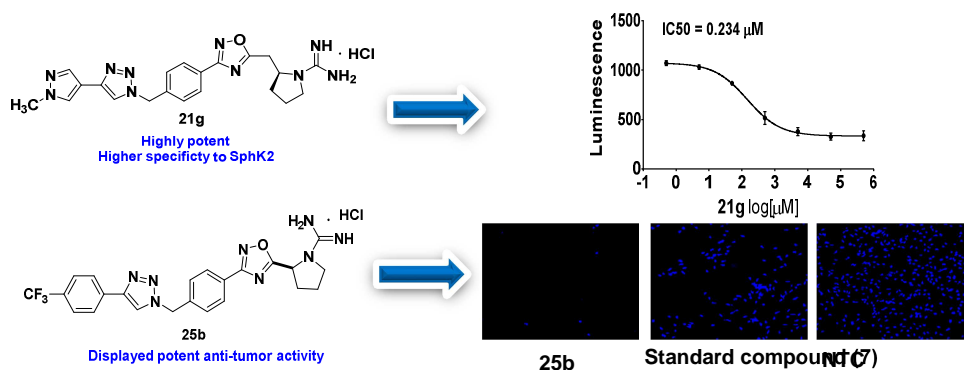
<sup>b</sup> Department of Radiology, Perelman School of Medicine, University of Pennsylvania, Philadelphia, Pennsylvania 19104, USA.

<sup>c</sup> Department of Surgery, University of Cincinnati, Cincinnati, Ohio 45267, USA

<sup>d</sup> Department of Radiation Oncology, Washington University School of Medicine, St. Louis, Missouri 63110, USA.

<sup>e</sup> Departments of Neurology, Neuroscience, Physical Therapy and Occupational Therapy, Washington University School of Medicine, St Louis, Missouri 63110, USA.

A novel class of new selective SphK2 inhibitors have been identified. Compound **21g** displayed the highest SphK2 inhibitory activity, and compound **25b** exhibited highest anti-tumor activity against human malignant glioblastoma tumor U-251 MG cell line.



## **Structure-activity relationship studies and bioactivity evaluation of 1,2,3-triazole containing analogues as a selective sphingosine kinase-2 inhibitors**

Vijai Kumar Reddy Tangadanchu <sup>a</sup>, Hao Jiang <sup>a</sup>, Yanbo Yu <sup>a</sup>, Thomas J. A. Graham <sup>b</sup>, Hui Liu <sup>c</sup>, Buck E. Rogers <sup>d</sup>, Robert Gropler <sup>a</sup>, Joel Perlmutter <sup>a,e</sup>, Zhude Tu <sup>a,\*</sup>

<sup>a</sup> Department of Radiology, Washington University School of Medicine, St. Louis, Missouri 63110, USA.

<sup>b</sup> Department of Radiology, Perelman School of Medicine, University of Pennsylvania, Philadelphia, Pennsylvania 19104, USA.

<sup>c</sup> Department of Surgery, University of Cincinnati, Cincinnati, Ohio 45267, USA.

<sup>d</sup> Department of Radiation Oncology, Washington University School of Medicine, St. Louis, Missouri 63110, USA.

<sup>e</sup> Departments of Neurology, Neuroscience, Physical Therapy and Occupational Therapy, Washington University School of Medicine, St Louis, Missouri 63110, USA.

Total Pages: 53

Schemes: 3

Tables: 3

Figures: 7

\*Address correspondence to:

Zhude Tu, Ph.D.  
Department of Radiology  
Washington University School of Medicine  
Campus Box 8225  
510 S. Kingshighway Blvd.  
St. Louis, MO 63110, USA  
Tel: 1-314-362-8487  
Fax: 1-314-362-8555  
E-mail: tuz@mir.wustl.edu

## Abstract

Sphingosine kinase (SphK) is primarily responsible for the production of Sphingosine-1-phosphate (S1P) that plays an important role in many biological and pathobiological processes including cancer, inflammation, neurological and cardiovascular disorders. Most research has focused on developing inhibitors of SphK1 rather than inhibitors of the other isoform SphK2 which has great importance in several pathophysiologic pathways. Exploration of new analogues for improving the potency and selectivity of SphK2 is highly demand. We now have designed, synthesized, and evaluated eighteen new 1,2,3-triazole analogues for their SphK2 inhibitory activity using a ADP-Glo kinase assay and their *in vivo* anti-tumor bioactivity. Several compounds including **21c**, **21e**, **21g**, **25e-h**, **29a-c** have high selectivity for SphK2 over SphK1; compound **21g** displayed the highest potency with an IC<sub>50</sub> value of 0.23 μM. In addition, three compounds **21a**, **21b**, and **25b** have the highest anti-tumor activity on cell viability against U-251 MG human glioblastoma cells. Molecular modeling study was performed to elucidate that polar head group and 1,2,3-triazole pharmacophore impact on the SphK2 selectivity.

**Keywords:** Sphingosine kinase 2 inhibitors, 1,2,3-Triazole hybrids, Selectivity, Molecular docking, ADP-Glo, U-251 MG Human glioblastoma cell.

---

\*Corresponding author. Tel.: +1 314 362 8487; fax: +1 314 362 8555.

*E-mail:* tuz@mir.wustl.edu (Z. Tu).

## 1. Introduction

In the past twenty years, significant strides have been made targeting the sphingolipid signaling as a therapeutic strategy due to its involvement in a wide range of cellular processes. The natural bioactive lipid mediator, sphingosine 1-phosphate (S1P) is a ubiquitous cellular signaling molecule that acts as a critical regulator of many physiological and pathophysiological processes related to, multiple sclerosis [1], Alzheimer disease [2, 3], cancer [4-7], and viral infections such as Chikungunya virus [8]. In particular, S1P affects proliferation, angiogenesis, and cell survival [9, 10]. The balance between S1P and pro-apoptotic ceramide plays an important role in numerous cancers such as non-small cell lung cancer, gastrointestinal cancer, and glioblastoma [11, 12].

Sphingosine kinase (SphK) is an important metabolic enzyme that catalyzes the phosphorylation of sphingosine to produce S1P. It plays a pivotal role in the regulation of numerous biological processes through the balance between S1P and ceramides. SphKs exist in two isoforms, SphK1 and SphK2. While SphK1 is 270 amino acids shorter than SphK2, they share approximately 50% sequence identity and the overlapping regions of these two proteins are highly conserved (**Supplemental Fig 1**). On the other hand, these two isoforms differ in cellular localization and degree of substrate selectivity [13, 14]. In fact, cellular functions of the two isoforms could vary depending on their subcellular localization. SphK1 is a cytosolic enzyme that promotes cell survival and proliferation [15, 16], whereas some SphK2 resides in the nucleus [17, 18], but can relocate to the cytosol on phosphorylation [19, 20]. Depending on the subcellular localization, SphK2 can promote either apoptosis or cell proliferation [8, 21]. Due to the critical roles of SphKs in the cell and the importance of the S1P metabolic pathway in various diseases, investigators have focused on the development of dual and specific SphK inhibitors as a complementary therapeutic strategy. For example, a specific potent SphK1 inhibitors may provide a therapeutic for oncology [6], whereas, recent studies have just begun to explore the role of SphK2 [22]. Therefore, identification of highly potent and selective SphK2 inhibitors would be of great value as

pharmacological tools to complement ongoing molecular and genetic studies. Such inhibitors will help unravel the roles of SphK2 in different pathophysiological conditions and explore potential therapeutic applications by targeting SphK2.

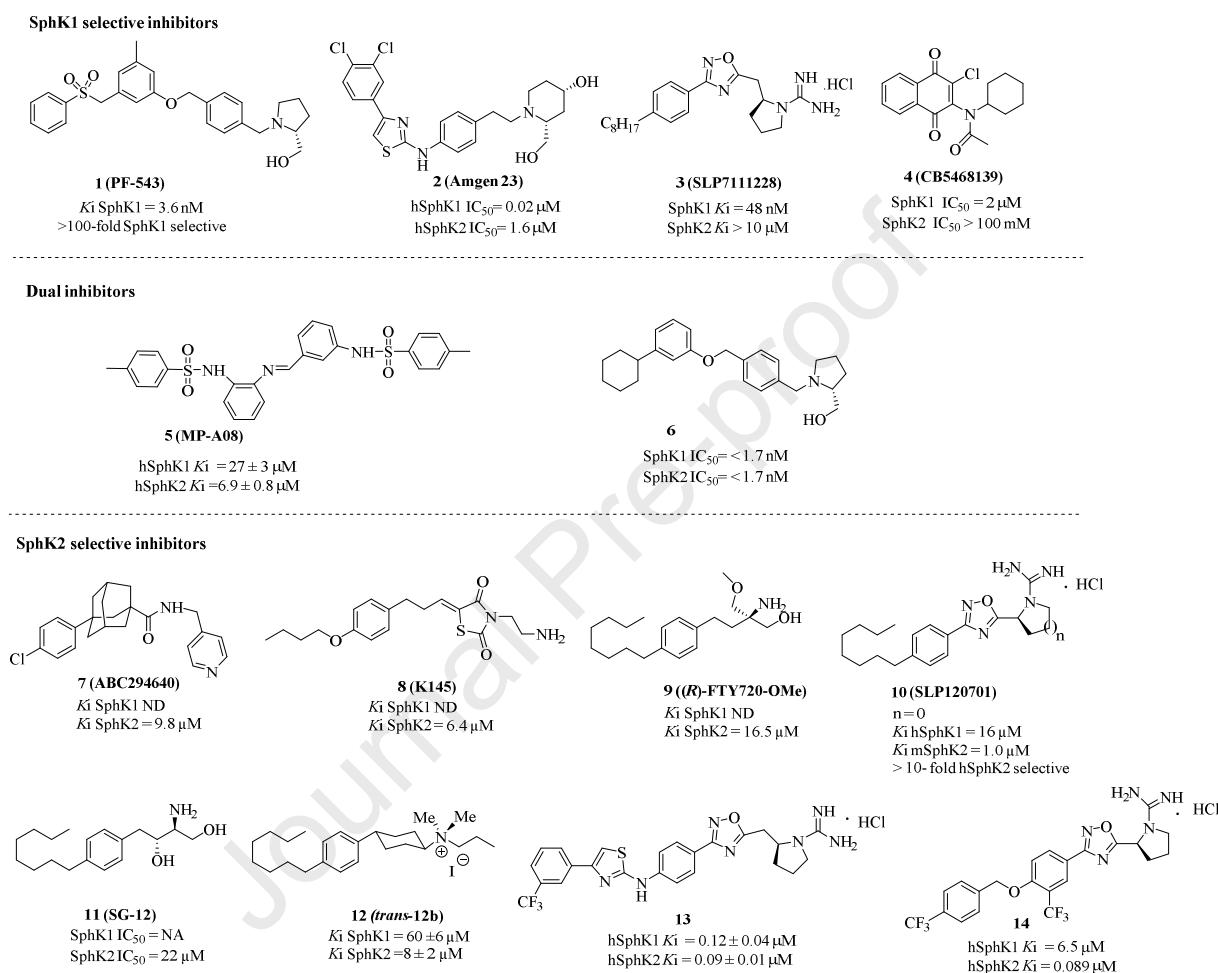


**Fig. 1.** Representative SphK1, dual SphK1/2, SphK2 inhibitors, and their inhibitory activities.

There are numeric reports of potent SphK1-selective inhibitors and SphK1/SphK2-dual inhibitors (**Fig. 1**). For example, Compound **1** (PF543,  $K_i$  = 3.6 nM, > 100 fold selective), **2** (Amgen 23), **3** (SLP7111228), **4** (CB5468139) are the most potent and selective SphK1 inhibitors, and these ligands provided as valuable molecular tools to investigate the S1P pathway [23-25]. Pitson and his colleagues have reported compound **5** (MP-A08) with  $K_i$  values of  $27 \pm 3$   $\mu$ M and  $6.9 \pm 0.8$   $\mu$ M against human SphK1 and SphK2, respectively [26]. Compound **6** is another potent dual inhibitor developed by

Schnute and coworkers at Pfizer [27] with an  $IC_{50}$  value of  $<1.7$  nM for both SphK1 and SphK2. Nevertheless, only a limited SphK2 inhibitors had been reported with moderate or low selectivity and potency. For example, compound **7** (ABC294640) [28], which is currently in phase II clinical trials for the treatment of pancreatic cancer and solid tumors (NCT01488513), exhibits moderate inhibitory activity and selectivity towards SphK2 ( $IC_{50}$ : SphK2  $\approx 60$   $\mu$ M; SphK1  $\geq 100$   $\mu$ M). Other SphK2 selective inhibitors have been reported, including **8** (K145) [29], **9** ((*R*)-FTY720-OMe) [30], and **10** (SLP120701) [25], **11** (SG-12) [31], **12** (*trans*-12b) [32], compound **13** [33], and compound **14** [34]. Therefore, new and adaptable chemical scaffolds for selective SphK2 inhibitors will help identifying the structural requirements for designing new SphK2 inhibitors and investigating their biological functions.

The lack of a small molecules having highly potent ( $<100$  nM) and selective ( $>100$ -fold) SphK2 inhibition prompted our interest to develop improved selective SphK2 inhibitors. Herein, we reported our efforts to explore a novel scaffold SphK2-selective inhibitors including design, synthesis, biological evaluation, molecular docking and structure-activity relationship analysis of the most potent SphK2-selective inhibitors described to date. All synthesized target compounds were fully characterized by  $^1$ H-NMR,  $^{13}$ C-NMR, and HRMS analysis. Our data suggested that several lead compounds exhibit relative high potency and high selectivity for SphK2.

## 2. Results and discussion

### 2.1. Design and development of selective SphK2 inhibitors

We designed a series of new SphK2 inhibitors (**Fig. 2B**) based on the structure activity relationship (SAR) analysis of reported data [33, 34], as well as the reported lead structures of the SphK2 inhibitors shown in **Fig. 1**. Santos et al. recently reported SphK2-selective inhibitors **13**, and **14** with  $K_i$  values of either 90 nM, or 89 nM [33, 34]. The inclusion of a methylene unit between the 1,2,4-oxadiazole and head group pyrrolidinyl rings provided a key factor for the inhibitor's selectivity.

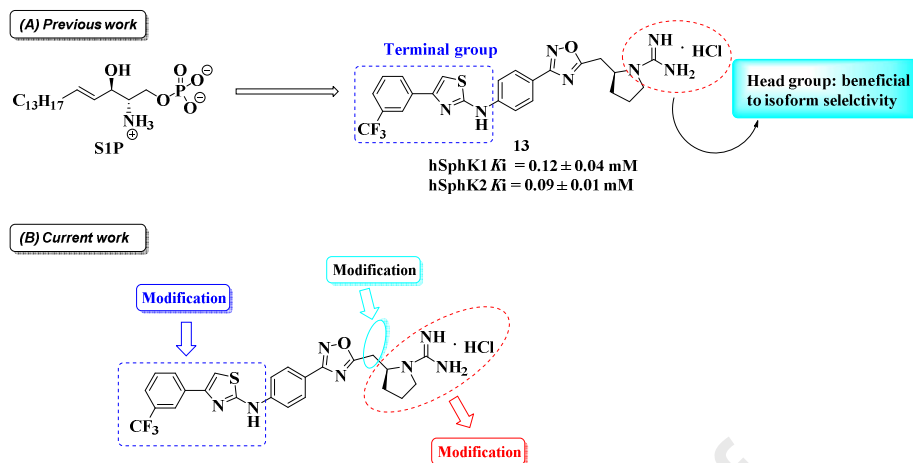


**Fig. 2.** Head and terminal group modifications towards the development of novel SphK2 inhibitors.

The authors also investigated the effects of different substituents on the phenyl ring in the terminal region by interposing the “aminothiazole terminal” linkage to an oxadiazole phenyl ring. Apparently, positioning of substituents attached to terminal region affected the SphK2 potency and selectivity. Using these strategies, we have designed and prepared a series of new derivatives by incorporating a 1,2,3-triazole pharmacophore to replace aminothiazole terminal with diverse aryl structures. Further, we focused on optimizing the head region of the base structure. Hence, the inclusion/exclusion of methylene unit and guanidino groups in compounds **13** & **14**, prompted us to design derivatives **21a-g**, **25a-h**, and **29a-c** (**Fig. 3**) bearing guanidino, and amidino motifs as the polar head substituents.

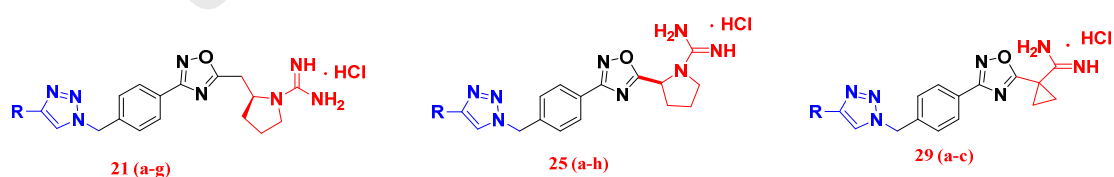
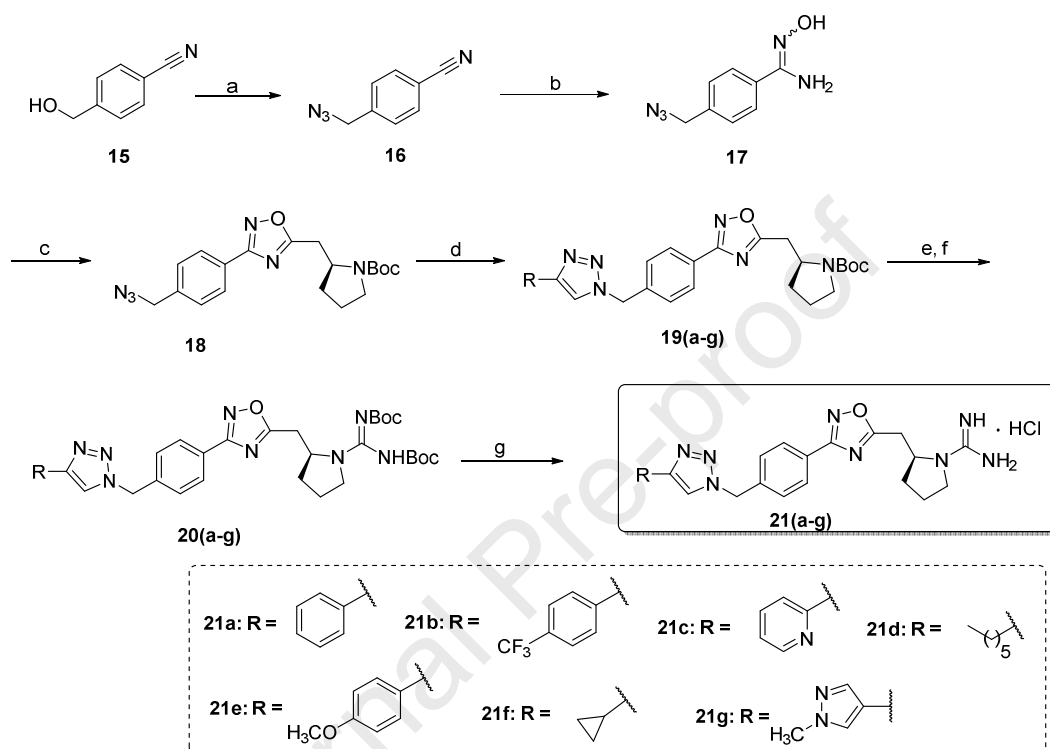


**Fig. 3.** Design of novel 1,2,3-triazole based SphK2 selective inhibitors.

## 2.2. Synthesis of SphK2 inhibitors

Guanidine, 1,2,4-oxadiazole, and internal phenyl ring moieties reportedly were key features of the sphingosine kinase inhibitor scaffold [33, 34]. Therefore, in the present study we focused our attention on the terminal region by appending 1,2,3-triazole pharmacophore to replace aminothiazole with diverse

aryl structures, to study the structure activity relationship. We made a few modifications based on the reported structure of the potent compound **13** to develop new SphK2 selective ligands. The synthesis of various substituted 1,2,3-triazole based SphK2 inhibitors as depicted in **Scheme 1**.

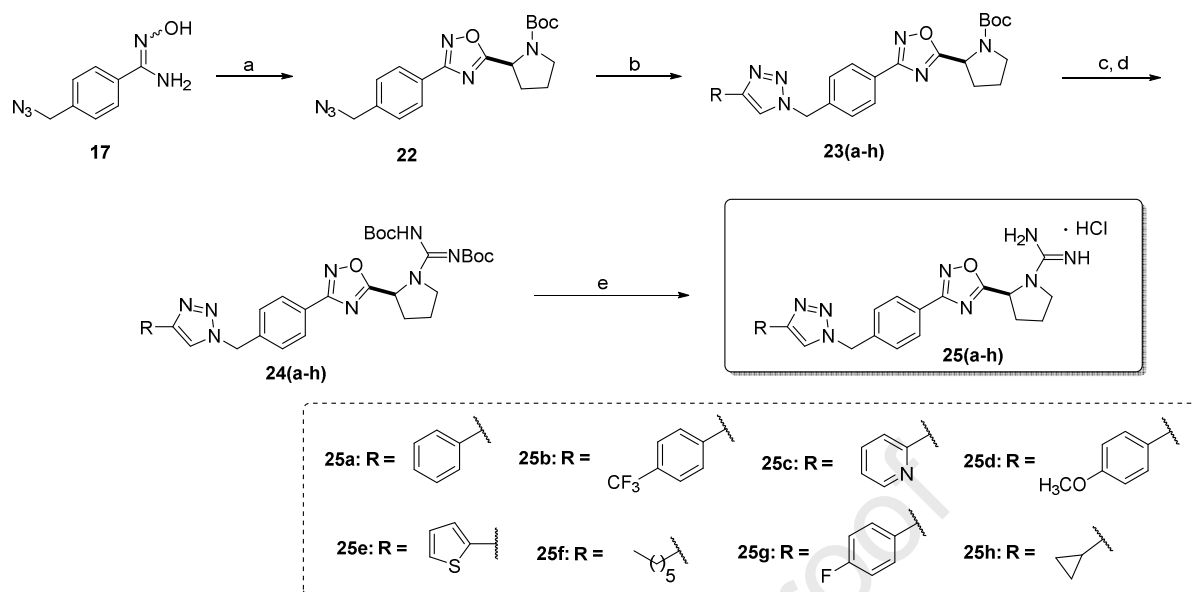


**Scheme 1.** Synthesis of target compounds **21a-g**. Reagents and conditions: (a) DPPA, toluene, rt, 12 h; (b) hydroxylamine hydrochloride, NaHCO<sub>3</sub>, CH<sub>3</sub>OH, reflux, 8 h; (c) Boc-*L*-homoproline, HCTU, DIPEA, DMF, rt to 100 °C, 10 h; (d) Substituted alkynes, 1:1 CH<sub>2</sub>Cl<sub>2</sub>:H<sub>2</sub>O, CuSO<sub>4</sub>·5H<sub>2</sub>O, (+)-Sodium *L*-ascorbate, rt, 12 h; (e) 1:1 TFA: CH<sub>2</sub>Cl<sub>2</sub>, rt, 6 h; (f) *N,N*-di-Boc-1*H*-pyrazole-1-carboxamide, DIPEA, CH<sub>3</sub>CN, 50 °C, 10 h; (g) 4N HCl, CH<sub>3</sub>OH, rt, 3 h.

The synthesis of 1,2,3-triazole containing new SphK2 inhibitors commenced from commercially available 4-(hydroxymethyl)benzonitrile **15**. The alcohol functionality was then transformed into azide **16** under the condition of 1,8-diazabicyclo [5.4.0]undec-7-ene (DBU) and diphenyl phosphoryl azide (DPPA) in 93% yield. 4-(Azidomethyl)benzonitrile **16** was then treated with hydroxylamine hydrochloride and sodium bicarbonate as a base in methanol under reflux conditions to yield amidoxime **17**, which is further reacted with homoproline using HCTU and Hunig's base at ~100 °C to afford the 1,2,4-oxadiazole moiety **18** with 56% yield.

Our next concern was the divergent synthesis of 1,2,3-triazole based SphK2 inhibitors using **18** as a building block. A copper catalyzed version of the Huisgen azide-alkyne cycloaddition protocol was employed to synthesize these triazole compounds. According to Huisgen's protocol [35], the click reaction between compound **18** with different alkynes, namely phenyl acetylene (**19a**), 1-ethynyl-4-(trifluoromethyl)benzene (**19b**), 2-ethynylpyridine (**19c**), hex-1-yne (**19d**), 1-ethynyl-4-methoxybenzene (**19e**), ethynylcyclopropane (**19f**), and 4-ethynyl-1-methyl-1*H*-pyrazole (**19g**) in presence of CuSO<sub>4</sub>·5H<sub>2</sub>O and sodium ascorbate as a reducing agent using a mixture of DCM:H<sub>2</sub>O (1:1, v/v) furnished the corresponding 1,2,3-triazole analogs with moderate to good isolated yields (45-89%) [36]. The Boc group in all the above compounds was removed with trifluoroacetic acid and successively reacted with *N,N*-di-Boc-1*H*-pyrazole-1-carboxamide in presence of Hunig's base in acetonitrile at 50 °C to afford di-Boc-protected guanidines **20a-g** in low yields. Finally, the desired target compounds had been successfully achieved by removal of di-Boc group using 4N HCl solution in dioxane. The desired guanidine based 1,2,3-triazoles derivatives **21a-g** were generated with good yields (65-91%) and further characterized by <sup>1</sup>H NMR, <sup>13</sup>C NMR, and HRMS analysis.

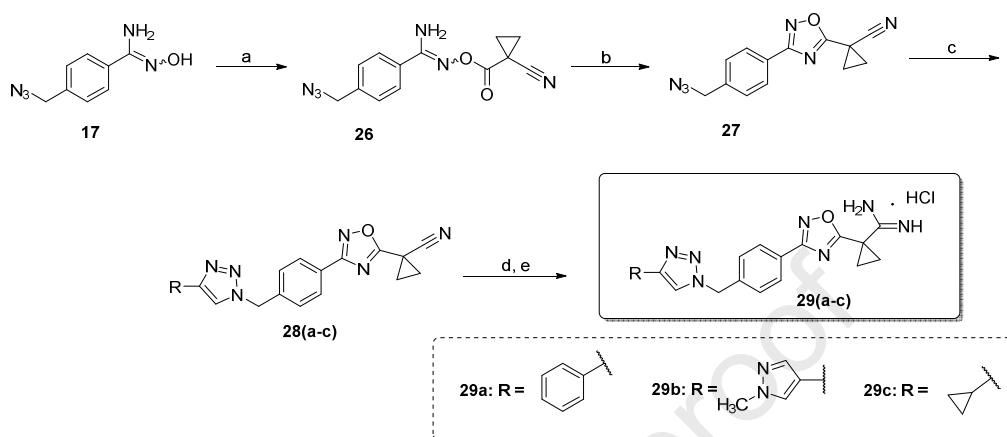
We made some modifications based on **Scheme 1** to develop additional new ligands for SphK2. We replaced the homoproline motif on the right side of the base structure with proline, while keeping the same 1,2,3-triazole pharmacophore on the left side, to study the structure activity relationship. We synthesized various substituted 1,2,3-triazole based SphK2 inhibitors as outlined in **Scheme 2**. Moving forward with our proposed strategy, the synthesis of target compounds **25a-h** was initiated with intermediate **17**, which is reacted with Boc-*L*-proline in presence of HCTU and Hunig's base at 100 °C to afford the 1,2,4-oxadiazole moiety **22** with high yield (89%).



**Scheme 2.** Synthesis of target compounds **25a-h**. Reagents and conditions: (a) Boc-*L*-proline, HCTU, DIPEA, DMF, rt to 100 °C, 10 h; (b) Substituted alkynes, 1:1 CH<sub>2</sub>Cl<sub>2</sub>:H<sub>2</sub>O, CuSO<sub>4</sub>·5H<sub>2</sub>O, (+)-Sodium *L*-ascorbate, rt, 12 h; (c) 1:1 TFA: CH<sub>2</sub>Cl<sub>2</sub>, rt, 6 h; (d) *N,N'*-di-Boc-1*H*-pyrazole-1-carboxamide, DIPEA, CH<sub>3</sub>CN, 50 °C, 10 h; (e) 4N HCl, CH<sub>3</sub>OH, rt, 3 h.

The next concern was the divergent synthesis of 1,2,3-triazole based SphK2 inhibitors using **22** as a building block. According to Huisgen's protocol, the click reaction between compound **22** with different alkynes, namely phenyl acetylene (**23a**), 1-ethynyl-4-(trifluoromethyl)benzene (**23b**), 2-ethynylpyridine (**23c**), 1-ethynyl-4-methoxybenzene (**23d**), 2-ethynylthiophene (**23e**), hex-1-yne (**23f**), 1-ethynyl-4-fluorobenzene (**23g**), and ethynylcyclopropane (**23h**), in presence of CuSO<sub>4</sub>·5H<sub>2</sub>O and sodium ascorbate as a reducing agent furnished the corresponding 1,2,3-triazole analogs in good isolated yields (56-85%). The Boc group in all the above compounds was removed with trifluoroacetic acid and successively reacted with *N,N*-di-Boc-1*H*-pyrazole-1-carboxamide in the presence of Hunig's base in acetonitrile at 50 °C to afford bis-Boc-protected guanidines in low yields. Finally, the desired target compounds **25a-h** had been successfully achieved by the removal of the di-Boc group with 4N HCl solution in dioxane afforded the desired guanidine based 1,2,3-triazoles derivatives in good yields (51-89%).

Our next design was to modify the polar head group using amidine motif. Once again, we utilized the key intermediate **17** to synthesis of amidine based 1,2,3-triazole target compounds **29a-c** (Scheme 3).



**Scheme 3.** Synthesis of target compounds **29a-c**. Reagents and conditions: (a) 1-cyanocyclopropanecarboxylic acid, PyBop, DIPEA, CH<sub>2</sub>Cl<sub>2</sub>, rt, 4 h; (b) TBAF, THF, rt, 2 h; (c) Substituted alkynes, 1:1 CH<sub>2</sub>Cl<sub>2</sub>:H<sub>2</sub>O, CuSO<sub>4</sub>·5H<sub>2</sub>O, (+)-Sodium *L*-ascorbate, rt, 12 h; (d) NaOMe, CH<sub>3</sub>OH, 50 °C, 24 h; (e) NH<sub>4</sub>Cl, 50 °C, 1 h.

Compound **17** was coupled with 1-cyano-1-cyclopropanecarboxylic acid by employing PyBOP to yield amidoxime compound **26**. Cyclization of the coupled amidoxime **26** with tetra-*n*-butylammonium fluoride (TBAF) gave oxadiazole **27** in 67% yield. We then synthesized the amidine based 1,2,3-triazole SphK2 inhibitors employing **27** as a building block. Again, the click reaction was conducted between **27** with different alkynes in presence of CuSO<sub>4</sub>·5H<sub>2</sub>O and sodium ascorbate as a reducing agent afforded the corresponding 1,2,3-triazole analogues **28a-c** in good isolated yields (62-85%). All the above synthesized 1,2,3-triazoles were further subjected to base-catalysed Pinner conditions [37] to yield the corresponding desired target compounds as amidines **29a-c** in moderate yields (51-59%).

### 2.3. *In vitro* SphK inhibitory activity evaluation and structure-activity relationship analysis

We sought to discover compounds with high potency and high selectivity for SphK2. Therefore, we first compared the inhibition activity of our synthesized compounds with the recent reported potent compound **13** [33] against both SphK1 and SphK2 using ADP-Glo Kinase Assay (Promega, Madison,

WI). Traditional lipid kinase assays rely on quantifying the amount of phosphate transfer to lipids using lipid extraction and thin-layer chromatography [22, 25, 38]. Although these assays are relative sensitivity and reliable, it is very challenging to separate the product from substrate. They are also expensive and labour-intensive, and difficult to use for high-throughput screening. Another method such as anti- Adenosine Diphosphate (ADP) antibody based assay can be easily used for high-through put screening, but has low dynamic range and limited sensitivity when the concentration of Adenosine Triphosphate (ATP) is too low [39].

The bioluminescence-based kinase assay such as ADP-Glo assay measures ADP formed from a kinase reaction with a luciferase. Upon the completion of a kinase reaction, the remaining ATP is depleted, the ADP produced in the kinase reaction is then converted to ATP and the detection is based on a sensitive and robust bioluminescence reaction. It has a broad linear range of ATP concentrations and high dynamic range. To determine the inhibition activity of our compounds, we used the ADP-Glo kinase assay which was able to detect down to 20% of 1  $\mu$ M ATP to ADP conversion (**Fig. 4A**).

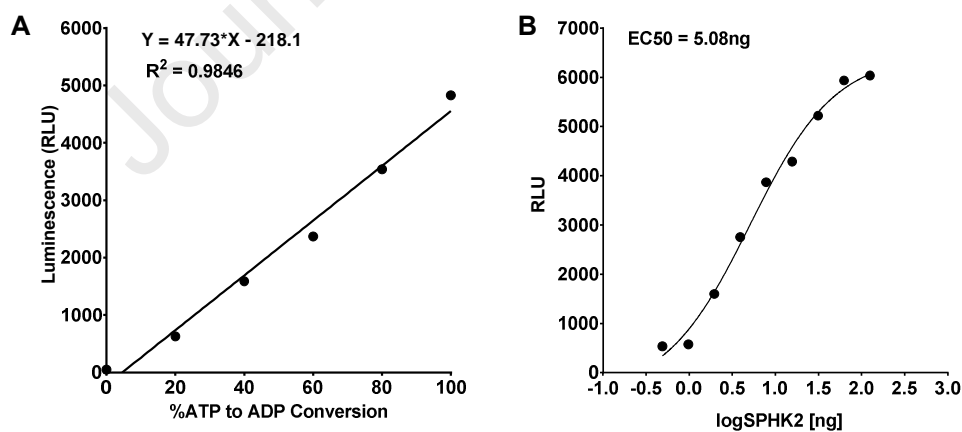


**Fig. 4.** Evaluation of ADP-Glo kinase assay performance using recombinant human SphK2. (A) ATP-ADP conversion curve. ATP to ADP standard curves were generated in the kinase buffer to evaluate the linearity of the assay and to determine the amount of ADP produced from each tested condition; (B) Human recombinant SphK2 showed a dose-response ATP to ADP conversion activity with an EC<sub>50</sub> of 5.08 ng.

It combines the sensitivity and throughput for the detection of ATP conversion, and provides a reliable method to determine the inhibition activity of chemical molecules toward purified kinase, such as SphK1 or SphK2. Today, the ADP-Glo kinase assay is widely used for library screening of kinase inhibitors [40], ATP/ADP metabolism and trafficking [41]. This assay is a convenient method for medium- and high-throughput screening and has an adequate sensitivity to determine the inhibitory activity for different kinase such as SphK1 and SphK2. In our studies, as shown in **Fig. 4B**, our data indicated that the recombinant human SphK2 has dose-response activity of ATP conversion with an  $EC_{50}$  of 5.08 ng. After incubation with optimizing concentration (125  $\mu$ M) of each synthesized compound, all compounds showed significant reduction of SphK2 activity as expected, with most of them showed more than a 50% reduction. Meanwhile, all new synthesized compounds only showed moderate to no effect on SphK1 activity (**Fig. 5**). The results indicated that all compounds are more favourable to inhibit SphK2 than SphK1 activity, and thus more selective to SphK2. Among all compounds, **21c**, **21e**, **21g**, **25e-h**, **29a-c** displayed the highest specificity to SphK2. In contrast, **21b**, **21d**, **21f**, and **25c** exhibited the lowest specificity to SphK2.

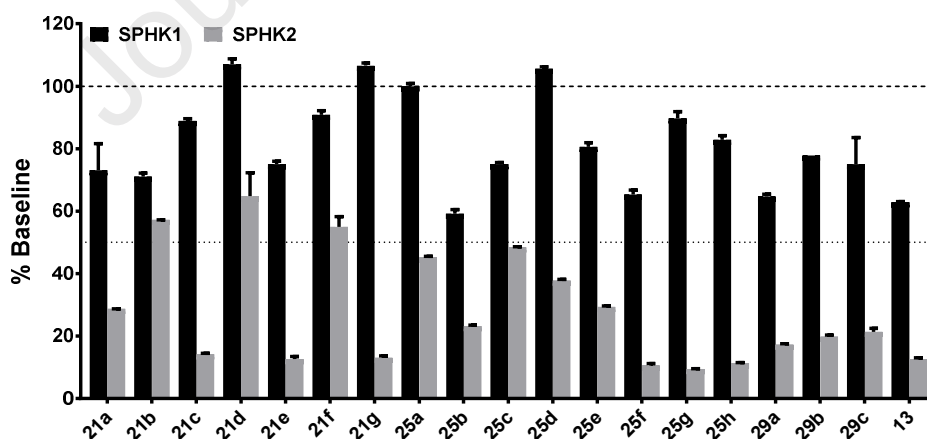
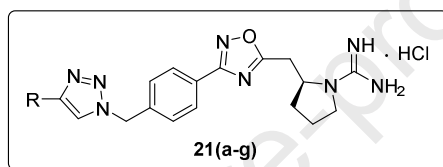


**Fig. 5.** The inhibition potency and selectivity of all new synthesized compounds toward SphK1 and SphK2 activity. The inhibitory activity of all compounds on SphK1 and SphK2 were measured using sphingosine kinase assays and presented as % baseline with no inhibitor added (no treatment control), 125  $\mu$ M of each compound were tested in triplicate, error bar indicates S.E. All tested new synthesized compounds showed high potency on

SphK2 inhibition (> 50% inhibition) and moderate to low potency on SphK1 inhibition (< 50% inhibition), indicated that these new compounds are selective for SphK2.

The IC<sub>50</sub> values of new compounds toward SphK2 using ADP-Glo assay were tabulated in **Table 1-3**. The results for derivatives **21a-g** bearing a 1,2,3-triazole at terminal region as well as a methylene linker between oxadiazole and a guanidine on the polar head are shown in **Table 1**. Compound **13** served as a reference standard compound for the inhibitory activity determination in our biological evaluation *in vitro* [33].

**Table 1.** SphK2 inhibitory activity of synthesized target compounds **21a-g**.



Compounds	R	SphK2 IC <sub>50</sub> (μM)	cLogP <sup>a</sup>
<b>21a</b>		0.396	1.97
<b>21b</b>		--	2.92
<b>21c</b>		0.452	0.86
<b>21d</b>		--	1.73
<b>21e</b>		0.640	1.96
<b>21f</b>		--	0.59
<b>21g</b>		0.234	0.17
<b>Compound 13 (std)</b>		0.280	5.18

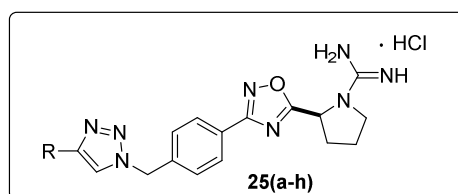
<sup>a</sup>cLogP was calculated from Chemdraw Professional 19.0; compound **13** served as a reference standard compound.

Our *in vitro* SphK2 inhibition data showed that compounds **21b**, **21d**, **21f** with a *para*-trifluoromethyl group of phenyl, butyl, and a cyclopropyl substituted groups on the 1,2,3-triazole terminal region, respectively, resulted no inhibitory activity, also no selective towards SphK2 (**Fig. 5**). In contrast, the compounds bearing a phenyl (**21a**), 2-pyridyl (**21c**), and *para*-methoxy group of phenyl (**21e**) substituted groups on the 1,2,3-triazole ring exhibited good to moderate inhibitory activities towards SphK2 with IC<sub>50</sub> values of 0.396 μM, 0.452 μM, 0.640 μM, respectively, when we compared with the standard reference compound (IC<sub>50</sub> = 0.28 μM). It is noteworthy that the compound having a 1-methylpyrazole substituted group on the 1,2,3-triazole terminal (**21g**), exhibited potent SphK2 inhibitory activity with an IC<sub>50</sub> value of 0.234 μM which was more potent compared to the reference compound **13** (IC<sub>50</sub> = 0.28 μM), and high selectivity for SphK2 over SphK1 (**Fig. 5**).

Our further exploration of new analogues focused on the polar head group without having a methylene linker between oxadiazole and guanidine motif, and the results are shown in **Table 2**. From one side, as shown in **Scheme 2**, we first retained a guanidine group on the polar head region, and studied the impact of various substituted groups on the 1,2,3-triazole terminal region **25a-h**. All synthesized analogues **25a-h** in this series had moderate to high potent SphK2 inhibitory activity, except compound **25a**. Particularly, compounds having heterocyclic substituents (**25c&e**) on the 1,2,3-triazole ring demonstrated moderate inhibition towards SphK2 with IC<sub>50</sub> values of 0.900 μM, 0.687 μM, respectively. A further improvement of SphK2 inhibitory activity was observed with the compounds bearing either an electron-donating (**25d**: IC<sub>50</sub> = 0.266 μM) or an electron-withdrawing substituted groups (**25b**: IC<sub>50</sub> = 0.359 μM; **25g**: IC<sub>50</sub> = 0.391 μM) on the aromatic ring of the 1,2,3-triazole terminal region. Interestingly, compounds containing non-aromatic substituents on the 1,2,3-triazole motif, such as compounds **25f&h** proved to be the most potent SphK2 inhibitors in this series with IC<sub>50</sub> values of 0.254

$\mu\text{M}$ , 0.248  $\mu\text{M}$ , respectively. In addition, these two compounds **25f&h** also displayed high selective for SphK2 over SphK1 (**Fig. 5**).

**Table 2.** SphK2 inhibitory activity of guanidine-based target compounds **25a-h**.

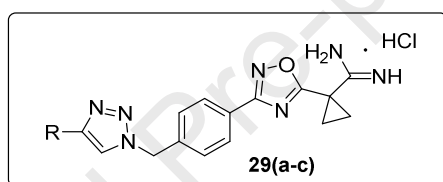


Compound	R	SphK2 IC <sub>50</sub> ( $\mu\text{M}$ )	cLogP <sup>a</sup>
<b>25a</b>		--	1.87
<b>25b</b>		0.359	2.82
<b>25c</b>		0.909	0.76
<b>25d</b>		0.266	1.86
<b>25e</b>		0.687	1.77
<b>25f</b>		0.254	1.63
<b>25g</b>		0.391	2.05
<b>25h</b>		0.248	0.49
<b>Compound 13 (std)</b>		0.280	5.18

<sup>a</sup>cLogP was calculated from Chemdraw Professional 19.0; compound **13** served as a reference standard compound.

We next investigated the impact of polar head group having an amidine motif, compounds **29a-c** were synthesized and evaluated for their *in vitro* SphK2 inhibitory activity, and the results are tabulated in **Table 3**. Pleasingly, we found that the introduction of an amidine polar head group containing 1,2,3-triazoles generally favoured SphK2 inhibition with higher selectivity over SphK1. For example, we observed better improvement in the inhibitory activities of compounds **29a**, and **29b** with an  $IC_{50}$  values of 0.261  $\mu$ M, 0.269  $\mu$ M respectively. However, compound **29c** bearing a cyclopropyl substitution on 1,2,3-triazole terminal displayed moderate inhibition ( $IC_{50} = 0.717 \mu$ M), in comparison to reference standard compound **13**.

**Table 3.** SphK2 inhibitory activity of amidine based target compounds **29a-c**.



Compound	R	SphK2 $IC_{50}$ ( $\mu$ M)	cLogP <sup>a</sup>
<b>29a</b>		0.261	1.49
<b>29b</b>		0.269	-0.31
<b>29c</b>		0.717	0.10
<b>Compound 13 (std)</b>		0.280	5.18

<sup>a</sup>cLogP was calculated from Chemdraw Professional 19.0; compound **13** served as a reference standard compound.

Finally, from the *in vitro* SphK2 inhibitory data shown in **Table 1-3**, we observed the following structure-activity relationship information: (a) an introduced methylene linker between oxadiazole and guanidine polar head group, most of the synthesized target compounds did not increase inhibition

towards SphK2, except compound **21g**; (b) excluding a methylene linker between oxadiazole and guanidine polar head group led to potent inhibition and higher selectivity of most compounds against SphK2. The inhibitory potency is as follows: non-aromatic > aromatic > heterocyclic substitutions on the terminal region; (c) further, introducing an amidine polar head group increased the inhibitory activity of compounds **29a** and **29b** with an  $IC_{50}$  values of 0.261  $\mu$ M, 0.269  $\mu$ M respectively with highly selective towards SphK2. The structure-activity relationship information of this newly synthesized scaffolds provides a valuable guide for the future design of new potent and selective SphK2 inhibitors.

#### 2.4. Modeling docking study

In addition to the SAR information derived from the medicinal chemistry efforts outlined above, we sought to evaluate potential binding modes for compound **29a** within SphK2 utilizing a combination of homology modeling and flexible receptor docking. Our approach was inspired by recent efforts that have enabled significant improvements in SphK2 inhibitor potency and selectivity [34]. Given the relative challenges of accurate homology modeling and ligand binding mode prediction, we sought to investigate the utility of modern tools for identifying possible binding modes for compound **29a** [42, 43]. Recently, significant advances have enabled more accurate prediction of protein structure determination *via* template-based methods through the use iterative Monte Carlo simulations and model refinement with molecular dynamics [44-46].

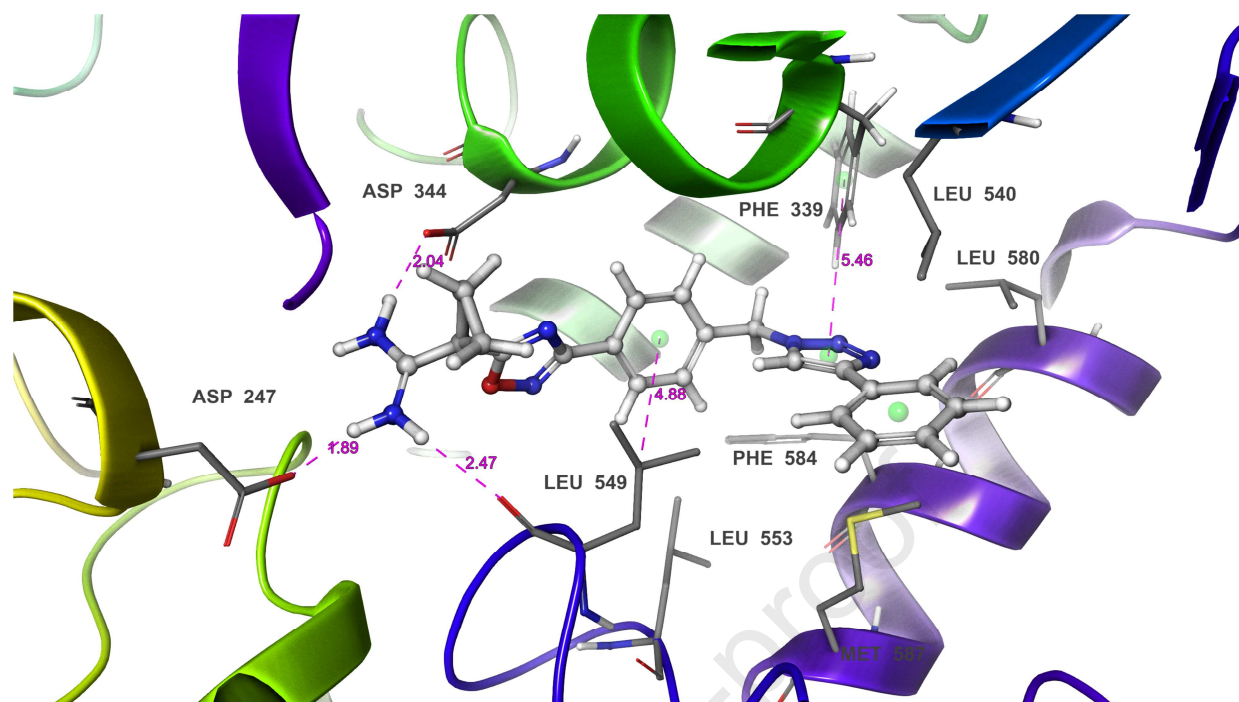


**Fig. 6.** Top-scoring binding pose of compound **29a** within the homology model of SphK2. Key interactions and their respective distances are highlighted in pink (distance is represented in angstroms).

Through the use of I-TASSAR, we constructed a full-length homology model of SphK2 that was then subjected to induced fit docking and metadynamics to identify likely binding poses for compound **29a** [47]. We opted to employ an approach that yielded a total of six high-scoring (IFD score) non-degenerate poses as identified by structural interaction fingerprints and following metadynamics, the top-scoring pose shown in **Fig. 6** (Pose Score) was selected for further analysis. The identified binding pose is comprised of key hydrogen bonding and electrostatic interactions between the polar amidine head piece of compound **29a** and Asp247, Asp344. Additionally, the amidine moiety of compound **29a** participates in a hydrogen bond with the amide backbone of Leu549 which may be further enabled by the methylene-cyclopropyl group found on compound **29a**. Contacts within the hydrophobic core and tail region are in line with previous observations and are comprised of hydrophobic and pi-pi interactions with Leu549, Leu540, Leu580, Phe339, and Phe584 [34]. Detailed analysis of

metadynamics trajectories for compound **29a** will be the subject of future studies. We anticipate that further refinement of this SphK2 model may enable the use of alchemical methods for free energy calculations with congeneric ligands [48].

### 2.5. *In vitro biological evaluation of antitumor activities*

Recently, increasing evidence indicates that SphK2 is involved in numerous diseases such as cancer. Inhibition of SphK2 showed promising anti-tumor effects in multiple cancers such as non-small cell lung cancer, gastrointestinal cancer, breast cancer, and prostate cancer [11]. It is proposed that SphK inhibitors can be used for treating malignant tumors such as glioblastoma [49], the most aggressive primary brain neoplasm with a median survival rate less than 1 year [50]. Targeting on SphK2 may provide an efficient and effective approach to the treatment of tumor, particularly for glioblastoma [51].

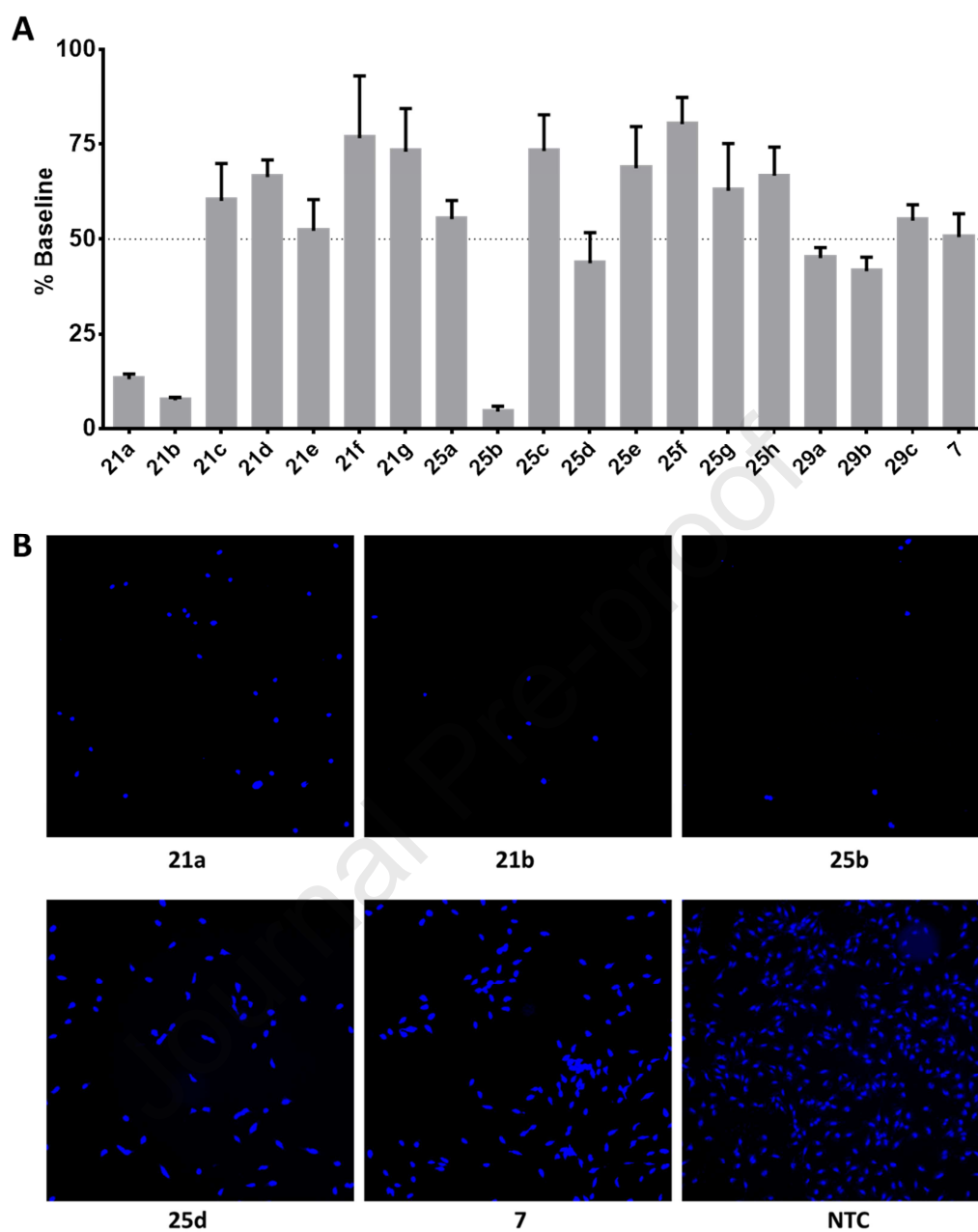


**Fig. 7.** The antitumor activity of new compounds on U-251 MG glioblastoma tumor cells. **(A)** The antitumor activities of all compounds on U-251 MG cell viability were measured and presented as % baseline with no inhibitor added. Each compound at concentration of 125  $\mu$ M was tested in triplicate, error bar indicates S.E. All tested compounds are able to reduce glioblastoma cell viability; three compounds **21a**, **21b**, and **25b** caused the significant reduction of glioblastoma cell viability, suggested three compounds had the strongest antitumor activity. **(B)** Representative images of Hoechst 33258 stained cells after the treatments from selected compounds.

Compound **7** (ABC294640) was reported as a well-known SphK2 selective inhibitor, and it is currently in phase II clinical trials for the treatment of pancreatic cancer and solid tumors through

various mechanisms [52, 53]. To evaluate the anti-tumor activity of these new SphK2 inhibitors, we compared the antitumor activities of our new compounds with compound **7** using a human malignant glioblastoma tumor derived U-251 MG cell line. After 24 hours incubation with 125  $\mu\text{M}$  of each compound, it was found that compound **7** reduced the cell viability of U-251 MG cells at approximately 50% as expected (**Fig. 7**), surprisingly, compounds **21a-b**, and **25b** were able to tremendously decrease the viability of U-251 MG cells at 125  $\mu\text{M}$  in 24 hours. Whereas compounds **21e**, **25d**, **29a-b** showed comparable reduction of viability of U-251 MG cells with compound **7**. This result suggests that our newly synthesized 1,2,3-triazole SphK2 inhibitors can potentially act as anti-tumor agents. At current stage, the clear pathway of these new compounds anti-tumor activity resulted solitary from the direct SphK inhibition of SphK2 or the combinations with facts is remain to be illustrated and further detail investigations will help the clarification.

### 3. Conclusion

In summary, we successfully designed and synthesized a series of new potent and selective SphK2 inhibitors. All synthesized scaffolds containing guanidine/amidine polar head and 1,2,3-triazole terminal groups. We further investigated the impact of modifying the polar head group as well as terminal region on the inhibitory activity and selectivity of these new compounds towards SphK2. All these target compounds were tested for *in vitro* SphK2 inhibitory activity using a ADP-Glo kinase assay, and antitumor activity using human malignant glioblastoma tumor derived U-251 MG cell line. The *in vitro* data suggested that compounds **21g**, **25d**, **25f**, **25h**, **29a**, and **29b** were potent towards SphK2 with  $\text{IC}_{50}$  values of 0.234, 0.266, 0.254, 0.248, 0.261, and 0.269  $\mu\text{M}$ , respectively. Compounds **21c**, **21e**, **21g**, **25e-h**, **29a-c** displayed high selectivity for SphK2 versus SphK1. Three compounds **21a-b**, and **25b** also exhibited higher antitumor activity for human malignant glioblastoma tumor U-251 MG cell line when compared with ABC294640. Molecular docking study revealed that polar head group plays an important role in the participation of hydrogen bonding, electrostatic interactions with Asp247, Asp344, and

Leu549. In addition, 1,2,3-triazole group fits securely into the hydrophobic “tail” region of the SphK2 binding site, thus might be leads to increased potency toward SphK2 with higher selectivity. Overall, our investigation provides a valuable information for further design and development of high potent and selective SphK2 inhibitors which may facilitate the development of therapeutics for treating diseases targeting on SphK2 and related sphingosine-mediated signaling.

## 4. Experimental

### 4.1. General

All reagents, and starting materials used in this study were obtained from commercial sources without any further purification. All dry reactions were conducted under a nitrogen atmosphere in oven dried glass apparatus using dry solvents. Yields refer to chromatographically, unless otherwise stated. Reactions were monitored by thin-layer chromatography (TLC) carried out on precoated glass plates of silica gel (0.25 mm) 60 F<sub>254</sub> from EMD Chemicals Inc. Visualization was accomplished with ultraviolet light (UV 254 nm), or by shaking the plate in a sealed jar containing silica gel and Iodine. Flash column chromatography was performed using Silia Flash® P60 40-63 $\mu$ m (230-400 mesh) from Silicycle. Melting points were determined on a MEL-TEMP 3.0 apparatus. <sup>1</sup>H NMR and <sup>13</sup>C NMR spectra were recorded on Varian 400 MHz (operating at 400 MHz for <sup>1</sup>H and 100 MHz for <sup>13</sup>C NMR) spectrometer. Rotamers are denoted by an asterisk (\*). Chemical shifts are reported in parts per million (ppm) and coupling constants *J* are given in Hz (Hertz). Chemical shifts are reported relative to TMS ( $\delta = 0.0$ ) as an internal standard. (Abbreviations used in spectra: s = singlet, d = doublet, t = triplet, q = quartet, m = multiplet, br = broad, dd = double of doublets, dt = doublet of triplets, td = triplet of doublets, qd = quartet of doublets). High resolution mass spectra (HRMS) [ESI]<sup>+</sup> were recorded on a Bruker MaXis 4G Q-TOF mass spectrometer with electrospray ionization source.

## 4.2. Chemistry

### 4.2.1. General procedure A: Coupling of amide-oxime derivatives with (S)-2-(1-(tert-butoxycarbonyl)pyrrolidin-2-yl)acetic acid/N-(tert-butoxycarbonyl)-L-proline

To a solution of (S)-2-(1-(tert-butoxycarbonyl)pyrrolidin-2-yl)acetic acid/N-(tert-butoxycarbonyl)-L-proline (1.1 equiv) in DMF (10 mL) was added DIPEA (1.8 equiv) and followed by addition of HCTU (1.5 equiv). The reaction mixture was stirred for 0.5 h followed by adding amidoxime (1.0 equiv). The reaction mixture was stirred for 1 h at room temperature, then stirred at 100 °C oil-bath for 8-10 h. The reaction progress was monitored by TLC. The solution was partitioned between EtOAc and LiBr aqueous solution. The aqueous solution was washed with EtOAc (3 × 10 mL), and the combined organic layers were washed with brine, dried over Na<sub>2</sub>SO<sub>4</sub>, filtered, and concentrated *via* vacuum. The resulting residue was purified by silica gel column chromatography.

### 4.2.2. General procedure B: Synthesis of 1,2,3-triazole derivatives

To a vigorously stirred solution of the azide (1 equiv) in DCM (5 mL) was added various terminal alkynes (1.1 equiv). The reaction was initiated by the addition of a solution of CuSO<sub>4</sub>·5H<sub>2</sub>O (0.01 equiv) and sodium ascorbate (0.1 equiv) in distilled water (5 mL). The coloured suspension that formed was stirred at room temperature for 10-12 h. The reaction progress was monitored by TLC. After completion of the reaction, the resulting mixture was diluted with CH<sub>2</sub>Cl<sub>2</sub> and then washed with brine. The combined organic extracts were dried over anhydrous Na<sub>2</sub>SO<sub>4</sub> and then concentrated under reduced pressure to afford crude product, which was purified by silica gel column chromatography to obtain pure 1,2,3-triazoles.

#### 4.2.3. General procedure C: Deprotection of *t*-Boc protecting groups with TFA and guanylation of amines

To a solution of azole based *t*-Boc-protected intermediates (1.0 equiv) in CH<sub>2</sub>Cl<sub>2</sub> (5 mL) was added a TFA (6.0 equiv) in CH<sub>2</sub>Cl<sub>2</sub> (5 mL). The reaction mixture was then stirred at rt for 4-6 h, and monitored *via* TLC. At this time, TLC showed complete conversion of the starting material. The organic solvent was removed under reduced pressure. The residue was then dissolved in CH<sub>3</sub>CN (10 mL). Diisopropylethylamine (10 equiv) and (*Z*)-*tert*-butyl (((*tert*-butoxycarbonyl)imino)(1*H*-pyrazol-1-yl)methyl)carbamate (1.1 equiv) were added to the above solution, and the resulting reaction mixture was stirred at 50 °C for 8-10 h, and monitored *via* TLC. Once the starting material was consumed, the solution was cooled to room temperature, and the solvent was removed under reduced pressure to afford the crude residue. The resulting residue was purified by silica gel column chromatography with 40-50% EtOAc in hexane to afford the desired 1,2,3-triazole based guanylated derivatives.

#### 4.2.4. General procedure D: Deprotection of *t*-Boc protecting groups with HCl

To a solution of *N*-Boc-protected compounds (1.0 equiv) in methanol (1 mL) was then added 4*N* hydrochloric acid (HCl) solution in dioxane (1 mL). The resulting reaction mixture was stirred for 2-3 h and monitored *via* TLC. Once the starting material was consumed, and the solvent was removed under reduced pressure to get the residue. The resulting residue was triturated with diethyl ether to yield the corresponding free amine hydrochloride salt.

#### 4.2.5. General procedure E: Conversion of nitriles to amidines

To a solution of a nitrile (1.0 eq.) in MeOH (0.10 M) was added a 0.5 M solution of sodium methoxide in MeOH (0.50 eq.) at rt and then heated to 50 °C for 24 h. The intermediate imidate was detectable by TLC; however, being in equilibrium with the nitrile, full conversion does not occur. Ammonium chloride (4.0 eq.) was then added in one portion at that temperature and allowed to react

until the imidate was completely consumed by TLC analysis. The reaction was then cooled to rt and evacuated to dryness to yield a crude solid. The solid was dissolved in minimum amount of water in order to remove excess ammonium chloride, and the solid was again evacuated to dryness. The crude solid material was then recrystallized in Et<sub>2</sub>O and DCM to yield the pure amidine hydrochloride salt. The yields varied greatly depending upon substrate, because amidine formation is dependent upon the equilibrium ratio between nitrile and imidate established under the sodium methoxide conditions.

#### 4.2.6.4-(Azidomethyl)benzonitrile (**16**)

To a round-bottom flask equipped with a stir bar was added 4-(hydroxymethyl)benzonitrile (5.0 g, 37.55 mmol), diphenyl phosphoryl azide (9.68 mL, 45.06 mmol), and toluene (25 mL). The mixture was cooled to 0 °C before adding 1,8- diazabicyclo [5.4.0]undec-7-ene (6.72 mL, 45.06 mmol) dropwise. The reaction was warmed to room temperature slowly and continued to stir for overnight. The reaction progress was monitored by TLC. After completion of the reaction, the resulting mixture was diluted with water (30 mL) and extracted with ethyl acetate (30 mL). The ethyl acetate layer was washed with 1M HCl, saturated brine and dried over anhydrous Na<sub>2</sub>SO<sub>4</sub>. The organic solvent was removed under reduced pressure. The crude residue was purified on a silica gel column chromatography, eluted with 10% EtOAc in hexane to afford the desired compound **16** (5.52 g, 93% yield) as a colorless solid. <sup>1</sup>H NMR (400 MHz, CDCl<sub>3</sub>) δ 7.65 (d, *J* = 8.3 Hz, 2H), 7.41 (d, *J* = 8.3 Hz, 2H), 4.42 (s, 2H).

#### 4.2.7.4-(Azidomethyl)-*N'*-hydroxybenzimidamide (**17**)

To a stirred suspension of NH<sub>2</sub>OH·HCl (4.39 g, 63.22 mmol) and NaHCO<sub>3</sub> (10.62 g, 126.44 mmol) in CH<sub>3</sub>OH (50 mL), a solution of **16** (5.0 g, 31.61 mmol) in CH<sub>3</sub>OH (10 mL) was gradually added. The reaction was refluxed and stirred in a pre-heated 75 °C oil-bath for 8 h. The reaction progress was monitored by TLC. After completion of the reaction, it was cooled to room temperature, and the precipitate was filtered off and washed with methanol. The filtrate was concentrated *in vacuo* without

further purification to afford **17** (5.50 g, 91% yield) as a white solid.  $^1\text{H}$  NMR (400 MHz, DMSO- $d_6$ )  $\delta$  9.68 (s, 1H), 7.71 (d,  $J = 8.2$  Hz, 2H), 7.37 (d,  $J = 8.2$  Hz, 2H), 5.83 (s, 2H), 4.46 (s, 2H).

4.2.8. *(S)-tert-Butyl-2-((3-(4-(azidomethyl)phenyl)-1,2,4-oxadiazol-5-yl)methyl)pyrrolidine-1-carboxylate (18)*

Synthesized by general procedure A: Yield: 56%; Pale yellow color solid;  $^1\text{H}$  NMR (400 MHz,  $\text{CDCl}_3$ )  $\delta$  8.08 (d,  $J = 8.2$  Hz, 2H), 7.41 (d,  $J = 8.0$  Hz, 2H), 4.40 (s, 2H), 4.28 (d,  $J = 24.9$  Hz, 1H), 3.45 – 3.28 (m, 3H), 3.15 – 2.98 (m, 1H), 2.12 – 2.03 (m, 1H), 1.90 – 1.78 (m, 3H), 1.45 (s, 9H).

4.2.9. *(S)-tert-Butyl-2-((3-(4-((4-phenyl-1H-1,2,3-triazol-1-yl)methyl)phenyl)-1,2,4-oxadiazol-5-yl)methyl)pyrrolidine-1-carboxylate (19a)*

Synthesized by general procedure B: Yield: 81%; White solid;  $^1\text{H}$  NMR (400 MHz,  $\text{CDCl}_3$ )  $\delta$  8.08 (d,  $J = 8.1$  Hz, 2H), 7.79 (d,  $J = 7.4$  Hz, 2H), 7.69 (s, 1H), 7.42 – 7.36 (m, 4H), 7.30 (t,  $J = 7.3$  Hz, 1H), 5.62 (s, 2H), 4.27 (d,  $J = 31.0$  Hz, 1H), 3.43–3.27 (m, 3H), 3.15 – 2.97 (m, 1H), 2.10 – 2.03 (m, 1H), 1.91 – 1.77 (m, 3H), 1.44 (s, 9H).

4.2.10. *(S)-tert-Butyl-2-((3-(4-((4-(4-(trifluoromethyl)phenyl)-1H-1,2,3-triazol-1-yl)methyl)phenyl)-1,2,4-oxadiazol-5-yl)methyl)pyrrolidine-1-carboxylate (19b)*

Synthesized by general procedure B: Yield: 45%; White solid;  $^1\text{H}$  NMR (400 MHz,  $\text{CDCl}_3$ )  $\delta$  8.09 (d,  $J = 8.2$  Hz, 2H), 7.90 (d,  $J = 8.1$  Hz, 2H), 7.76 (s, 1H), 7.64 (d,  $J = 8.2$  Hz, 2H), 7.40 (d,  $J = 8.0$  Hz, 2H), 5.64 (s, 2H), 4.27 (d,  $J = 31.4$  Hz, 1H), 3.45 – 3.27 (m, 3H), 3.12 – 2.98 (m, 1H), 2.09 – 1.99 (m, 1H), 1.89 – 1.77 (m, 3H), 1.44 (s, 9H).

4.2.11. *(S)-tert-Butyl-2-((3-(4-((4-(pyridin-2-yl)-1H-1,2,3-triazol-1-yl)methyl)phenyl)-1,2,4-oxadiazol-5-yl)methyl)pyrrolidine-1-carboxylate (19c)*

Synthesized by general procedure B: Yield: 78%; White solid;  $^1\text{H}$  NMR (400 MHz,  $\text{CDCl}_3$ )  $\delta$  8.51 (d,  $J = 4.8$  Hz, 1H), 8.15 (d,  $J = 7.9$  Hz, 1H), 8.10 – 8.03 (m, 3H), 7.74 (td,  $J = 7.6, 1.2$  Hz, 1H), 7.40 (d,  $J = 8.0$  Hz, 2H), 7.19 (dd,  $J = 6.6, 5.1$  Hz, 1H), 5.62 (s, 2H), 4.26 (d,  $J = 29.4$  Hz, 1H), 3.42 – 3.37 (m, 3H), 3.13 – 2.96 (m, 1H), 2.09 – 2.03 (m, 1H), 1.90 – 1.75 (m, 3H), 1.43 (s, 9H).

4.2.12. *(S)-tert-Butyl-2-((3-(4-((4-butyl-1H-1,2,3-triazol-1-yl)methyl)phenyl)-1,2,4-oxadiazol-5-yl)methyl)pyrrolidine-1-carboxylate (19d)*

Synthesized by general procedure B: Yield: 85%; White solid;  $^1\text{H}$  NMR (400 MHz,  $\text{CDCl}_3$ )  $\delta$  8.05 (d,  $J = 8.1$  Hz, 2H), 7.32 (d,  $J = 8.0$  Hz, 2H), 7.19 (s, 1H), 5.53 (s, 2H), 4.26 (d,  $J = 33.0$  Hz, 1H), 3.45 – 3.26 (m, 3H), 3.12 – 3.00 (m, 1H), 2.68 (t,  $J = 7.7$  Hz, 2H), 2.10 – 2.05 (m, 1H), 1.92 – 1.76 (m, 3H), 1.65 – 1.57 (m, 2H), 1.44 (s, 9H), 1.37 – 1.31 (q, 2H), 0.89 (t,  $J = 7.3$  Hz, 3H).

4.2.13. *(S)-tert-Butyl-2-((3-(4-((4-(4-methoxyphenyl)-1H-1,2,3-triazol-1-yl)methyl)phenyl)-1,2,4-oxadiazol-5-yl)methyl)pyrrolidine-1-carboxylate (19e)*

Synthesized by general procedure B: Yield: 57%; White solid;  $^1\text{H}$  NMR (400 MHz,  $\text{CDCl}_3$ )  $\delta$  8.11 (d,  $J = 8.2$  Hz, 2H), 7.75 (d,  $J = 8.8$  Hz, 2H), 7.64 (s, 1H), 7.42 (d,  $J = 8.0$  Hz, 2H), 6.96 (d,  $J = 8.8$  Hz, 2H), 5.64 (s, 2H), 4.31 (d,  $J = 36.5$  Hz, 1H), 3.85 (s, 3H), 3.46 – 3.32 (m, 3H), 3.16 – 3.02 (m, 1H), 2.13 – 2.04 (m, 1H), 1.93 – 1.78 (m, 3H), 1.48 (s, 9H).

4.2.14. *(S)-tert-Butyl-2-((3-(4-((4-cyclopropyl-1H-1,2,3-triazol-1-yl)methyl)phenyl)-1,2,4-oxadiazol-5-yl)methyl)pyrrolidine-1-carboxylate (19f)*

Synthesized by general procedure B: Yield: 89%; White solid;  $^1\text{H}$  NMR (400 MHz,  $\text{CDCl}_3$ )  $\delta$  8.11 (d,  $J = 8.1$  Hz, 2H), 7.38 (d,  $J = 8.0$  Hz, 2H), 7.22 (s, 1H), 5.57 (s, 2H), 4.33 (d,  $J = 27.4$  Hz, 1H), 3.53 – 3.34 (m, 3H), 3.23 – 3.04 (m, 1H), 2.14 – 2.11 (m, 1H), 2.00 – 1.88 (m, 4H), 1.50 (s, 9H), 1.02 – 0.94 (m, 2H), 0.89 – 0.85 (m, 2H).

4.2.15. *(S)*-*tert*-Butyl-2-((3-(4-((4-(1-methyl-1*H*-pyrazol-4-yl)-1*H*-1,2,3-triazol-1-yl)methyl)phenyl)-1,2,4-oxadiazol-5-yl)methyl)pyrrolidine-1-carboxylate (**19g**)

Synthesized by general procedure B: Yield: 51%; White solid; <sup>1</sup>H NMR (400 MHz, CDCl<sub>3</sub>) δ 8.11 (d, *J* = 7.9 Hz, 2H), 7.80 (s, 1H), 7.72 (s, 1H), 7.51 (s, 1H), 7.41 (d, *J* = 7.7 Hz, 2H), 5.62 (s, 2H), 4.30 (d, *J* = 27.6 Hz, 1H), 3.95 (s, 3H), 3.47 – 3.31 (m, 3H), 3.14 – 3.00 (m, 1H), 2.11 – 2.02 (m, 1H), 1.94 – 1.80 (br m, 3H), 1.47 (s, 9H).

4.2.16. *(S)*-*tert*-Butyl-(((*tert*-butoxycarbonyl)imino)(2-((3-(4-((4-phenyl-1*H*-1,2,3-triazol-1-yl)methyl)phenyl)-1,2,4-oxadiazol-5-yl)methyl)pyrrolidin-1-yl)methyl)carbamate (**20a**)

Synthesized by general procedure C: Yield: 51%; White solid; <sup>1</sup>H NMR (400 MHz, CDCl<sub>3</sub>) δ 10.27 (s, 1H), 8.10 (d, *J* = 8.0 Hz, 2H), 7.79 (d, *J* = 7.6 Hz, 2H), 7.67 (s, 1H), 7.39 (dd, *J* = 7.4, 5.1 Hz, 4H), 7.30 (t, *J* = 7.3 Hz, 1H), 5.62 (s, 2H), 4.77 – 4.73 (m, 1H), 3.66 – 3.59 (m, 2H), 3.50 – 3.41 (m, 1H), 3.19 – 3.13 (m, 1H), 2.27 – 2.20 (m, 1H), 1.91 – 1.87 (m, 1H), 1.82 – 1.73 (m, 2H), 1.44 (s, 18H).

4.2.17. *(S)*-*tert*-Butyl-(((*tert*-butoxycarbonyl)imino)(2-((3-(4-((4-(4-(trifluoromethyl)phenyl)-1*H*-1,2,3-triazol-1-yl)methyl)phenyl)-1,2,4-oxadiazol-5-yl)methyl)pyrrolidin-1-yl)methyl)carbamate (**20b**)

Synthesized by general procedure C: Yield: 60%; White solid; <sup>1</sup>H NMR (400 MHz, CDCl<sub>3</sub>) δ 10.38 (s, 1H), 8.19 (d, *J* = 7.8 Hz, 2H), 7.98 (d, *J* = 7.9 Hz, 2H), 7.83 (s, 1H), 7.72 (d, *J* = 8.0 Hz, 2H), 7.48 (d, *J* = 7.9 Hz, 2H), 5.72 (s, 2H), 4.85 – 4.82 (m, 1H), 3.71 (dd, *J* = 17.2, 7.9 Hz, 2H), 3.59 – 3.49 (m, 1H), 3.24 (dd, *J* = 14.4, 8.5 Hz, 1H), 2.34 – 2.27 (m, 1H), 1.98 – 1.94 (m, 1H), 1.90 – 1.81 (m, 2H), 1.52 (s, 18H).

4.2.18. (*S*)-*tert*-Butyl-(((*tert*-butoxycarbonyl)imino)(2-((3-(4-((4-(pyridin-2-yl)-1*H*-1,2,3-triazol-1-yl)methyl)phenyl)-1,2,4-oxadiazol-5-yl)methyl)pyrrolidin-1-yl)methyl)carbamate (**20c**)

Synthesized by general procedure C: Yield: 25%; White solid;  $^1\text{H}$  NMR (400 MHz,  $\text{CDCl}_3$ )  $\delta$  10.36 (s, 1H), 8.59 (d,  $J = 4.9$  Hz, 1H), 8.23 (d,  $J = 7.9$  Hz, 1H), 8.19 – 8.11 (m, 3H), 7.82 (t,  $J = 7.6$  Hz, 1H), 7.47 (d,  $J = 8.0$  Hz, 2H), 7.30 – 7.24 (m, 1H), 5.70 (s, 2H), 4.83 – 4.79 (m, 1H), 3.74 – 3.66 (m, 2H), 3.57 – 3.47 (m, 1H), 3.24 (dd,  $J = 17.7, 8.2$  Hz, 1H), 2.33 – 2.26 (m, 1H), 2.03 – 1.93 (m, 1H), 1.92 – 1.79 (m, 2H), 1.51 (d,  $J = 5.0$  Hz, 18H).

4.2.19. (*S*)-*tert*-Butyl-(((*tert*-butoxycarbonyl)imino)(2-((3-(4-((4-butyl-1*H*-1,2,3-triazol-1-yl)methyl)phenyl)-1,2,4-oxadiazol-5-yl)methyl)pyrrolidin-1-yl)methyl)carbamate (**20d**)

Synthesized by general procedure C: Yield: 33%; White solid;  $^1\text{H}$  NMR (400 MHz,  $\text{CDCl}_3$ )  $\delta$  10.34 (s, 1H), 8.12 (d,  $J = 8.0$  Hz, 2H), 7.37 (d,  $J = 8.1$  Hz, 2H), 7.24 (s, 1H), 5.58 (s, 2H), 4.82 – 4.76 (m, 1H), 3.68 (dd,  $J = 16.9, 9.6$  Hz, 2H), 3.55 – 3.49 (m, 1H), 3.21 (dd,  $J = 14.7, 8.0$  Hz, 1H), 2.74 (t,  $J = 7.7$  Hz, 2H), 2.33 – 2.26 (m, 1H), 2.01 – 1.92 (m, 1H), 1.88 – 1.81 (m, 2H), 1.70 – 1.64 (m, 2H), 1.50 (d,  $J = 9.0$  Hz, 18H), 1.40 (dd,  $J = 14.9, 7.4$  Hz, 2H), 0.95 (t,  $J = 7.3$  Hz, 3H).

4.2.20. (*S*)-*tert*-Butyl-(((*tert*-butoxycarbonyl)imino)(2-((3-(4-((4-(4-methoxyphenyl)-1*H*-1,2,3-triazol-1-yl)methyl)phenyl)-1,2,4-oxadiazol-5-yl)methyl)pyrrolidin-1-yl)methyl)carbamate (**20e**)

Synthesized by general procedure C: Yield: 22%; White solid;  $^1\text{H}$  NMR (400 MHz,  $\text{CDCl}_3$ )  $\delta$  10.32 (s, 1H), 8.13 (d,  $J = 8.0$  Hz, 2H), 7.75 (d,  $J = 8.7$  Hz, 2H), 7.63 (s, 1H), 7.42 (d,  $J = 8.0$  Hz, 2H), 6.96 (d,  $J = 8.7$  Hz, 2H), 5.64 (s, 2H), 4.85 – 4.74 (m, 1H), 3.85 (s, 3H), 3.72 – 3.62 (m, 2H), 3.20 (dd,  $J = 15.0, 8.2$  Hz, 1H), 2.31 – 2.25 (m, 1H), 1.99 – 1.75 (m, 4H), 1.48 (s, 18H).

4.2.21. *(S)*-*tert*-Butyl-(((*tert*-butoxycarbonyl)imino)(2-((3-(4-((4-cyclopropyl-1*H*-1,2,3-triazol-1-yl)methyl)phenyl)-1,2,4-oxadiazol-5-yl)methyl)pyrrolidin-1-yl)methyl)carbamate (**20f**)

Synthesized by general procedure C: Yield: 25%; White solid;  $^1\text{H}$  NMR (400 MHz,  $\text{CDCl}_3$ )  $\delta$  10.34 (s, 1H), 8.12 (d,  $J = 8.0$  Hz, 2H), 7.37 (d,  $J = 8.0$  Hz, 2H), 7.19 (s, 1H), 5.55 (s, 2H), 4.83 – 4.77 (m, 1H), 3.76 – 3.63 (m, 2H), 3.59 – 3.47 (m, 1H), 3.21 (dd,  $J = 14.7, 7.5$  Hz, 1H), 2.34 – 2.23 (m, 1H), 1.99 – 1.92 (m, 2H), 1.88 – 1.80 (m, 2H), 1.50 (s, 18H), 0.98 – 0.94 (m, 2H), 0.89 – 0.83 (m, 2H).

4.2.22. *(S)*-*tert*-Butyl-(((*tert*-butoxycarbonyl)imino)(2-((3-(4-((4-(1-methyl-1*H*-pyrazol-4-yl)-1*H*-1,2,3-triazol-1-yl)methyl)phenyl)-1,2,4-oxadiazol-5-yl)methyl)pyrrolidin-1-yl)methyl)carbamate (**20g**)

Synthesized by general procedure C: Yield: 19%; White solid;  $^1\text{H}$  NMR (400 MHz,  $\text{CDCl}_3$ )  $\delta$  10.34 (s, 1H), 8.14 (d,  $J = 8.0$  Hz, 2H), 7.82 (s, 1H), 7.74 (s, 1H), 7.53 (s, 1H), 7.42 (d,  $J = 8.0$  Hz, 2H), 5.64 (s, 2H), 4.86 – 4.76 (m, 1H), 3.97 (s, 3H), 3.74 – 3.64 (m, 2H), 3.58 – 3.47 (m, 1H), 3.23 – 3.16 (m, 1H), 2.34 – 2.24 (m, 1H), 1.99 – 1.82 (m, 3H), 1.53 – 1.45 (m, 18H).

4.2.23. *(S)*-2-((3-(4-((4-Phenyl-1*H*-1,2,3-triazol-1-yl)methyl)phenyl)-1,2,4-oxadiazol-5yl)methyl)pyrrolidine-1-carboximidamide hydrochloride (**21a**)

Synthesized by general procedure D: Yield: 85%; White solid;  $^1\text{H}$  NMR (400 MHz,  $\text{CD}_3\text{OD}$ )  $\delta$  8.56 (s, 1H), 8.11 (d,  $J = 8.2$  Hz, 2H), 7.82 (d,  $J = 7.3$  Hz, 2H), 7.57 (d,  $J = 8.2$  Hz, 2H), 7.46 (t,  $J = 7.4$  Hz, 2H), 7.39 (t,  $J = 7.4$  Hz, 1H), 5.79 (s, 2H), 4.53 (q,  $J = 7.5$  Hz, 1H), 3.76 – 3.66 (m, 1H), 3.60 – 3.41 (m, 3H), 2.33 – 2.22 (m, 1H), 2.16 – 2.01 (m, 3H);  $^{13}\text{C}$  NMR (101 MHz,  $\text{CD}_3\text{OD} + \text{DMSO-d}_6$ )  $\delta$  178.45, 168.96, 156.12, 148.84, 140.66, 131.88, 130.15, 129.91, 129.42, 128.96, 127.87, 126.68, 122.73, 56.86, 54.34, 48.83, 31.55, 30.08, 23.53; HRMS (ESI)  $m/z$   $[\text{M} + \text{H}]^+$  calcd. for  $\text{C}_{23}\text{H}_{25}\text{N}_8\text{O}$  429.2146, found 429.2149.

4.2.24. (*S*)-2-((3-(4-((4-(4-(Trifluoromethyl)phenyl)-1*H*-1,2,3-triazol-1-yl)methyl)phenyl)-1,2,4-oxadiazol-5-yl)methyl)pyrrolidine-1-carboximidamide hydrochloride (**21b**)

Synthesized by general procedure D: Yield: 89%; White solid;  $^1\text{H}$  NMR (400 MHz,  $\text{CD}_3\text{OD}$ )  $\delta$  8.57 (s, 1H), 8.09 (d,  $J = 8.0$  Hz, 2H), 8.02 (d,  $J = 8.1$  Hz, 2H), 7.73 (d,  $J = 8.1$  Hz, 2H), 7.54 (d,  $J = 8.1$  Hz, 2H), 5.77 (s, 2H), 4.57 – 4.49 (m, 1H), 3.68 – 3.42 (m, 3H), 3.32 (s, 1H), 2.31 – 2.23 (m, 1H), 2.16 – 1.98 (m, 3H);  $^{13}\text{C}$  NMR (101 MHz,  $\text{DMSO-d}_6$ )  $\delta$  177.70, 167.58, 155.08, 145.73, 139.68, 134.97, 133.69, 129.25, 128.64\*, 128.32\*, 127.95, 126.39, 126.35, 126.31, 126.14, 126.00\*, 123.57, 123.30\*, 105.42, 55.21, 53.16, 47.88, 30.39, 29.24, 22.49; HRMS (ESI)  $m/z$   $[\text{M} + \text{H}]^+$  calcd. for  $\text{C}_{24}\text{H}_{24}\text{F}_3\text{N}_8\text{O}$  497.2015, found 497.2014.

4.2.25. (*S*)-2-((3-(4-((4-(Pyridin-2-yl)-1*H*-1,2,3-triazol-1-yl)methyl)phenyl)-1,2,4-oxadiazol-5-yl)methyl)pyrrolidine-1-carboximidamide hydrochloride (**21c**)

Synthesized by general procedure D: Yield: 78%; White solid;  $^1\text{H}$  NMR (400 MHz,  $\text{CD}_3\text{OD}$ )  $\delta$  9.07 (s, 1H), 8.78 (d,  $J = 5.4$  Hz, 1H), 8.65 (t,  $J = 7.3$  Hz, 1H), 8.48 (d,  $J = 8.2$  Hz, 1H), 8.11 (d,  $J = 8.3$  Hz, 2H), 7.99 (t,  $J = 6.8$  Hz, 1H), 7.60 (d,  $J = 8.2$  Hz, 2H), 5.87 (s, 2H), 4.56 – 4.51 (m, 1H), 3.57 – 3.43 (m, 2H), 3.34 (d,  $J = 5.0$  Hz, 2H), 2.31 – 2.24 (m, 1H), 2.18 – 1.97 (m, 3H);  $^{13}\text{C}$  NMR (101 MHz,  $\text{DMSO-d}_6$ )  $\delta$  177.72, 167.56, 155.11, 146.54\*, 146.09, 142.54\*, 139.44, 129.35, 129.30\*, 128.06\*, 127.96, 126.47, 125.98, 124.91, 122.03, 55.20, 53.28, 47.88, 31.73\*, 30.39, 29.25, 22.50; HRMS (ESI)  $m/z$   $[\text{M} + \text{H}]^+$  calcd. for  $\text{C}_{22}\text{H}_{24}\text{N}_9\text{O}$  430.2098, found 430.2100.

4.2.26. (*S*)-2-((3-(4-((4-Butyl-1*H*-1,2,3-triazol-1-yl)methyl)phenyl)-1,2,4-oxadiazol-5-yl)methyl)pyrrolidine-1-carboximidamide hydrochloride (**21d**)

Synthesized by general procedure D: Yield: 89%; White solid;  $^1\text{H}$  NMR (400 MHz,  $\text{CD}_3\text{OD}$ )  $\delta$  8.36 (s, 1H), 8.12 (d,  $J = 8.1$  Hz, 2H), 7.58 (d,  $J = 8.1$  Hz, 2H), 5.83 (s, 2H), 4.59 – 4.48 (m, 1H), 3.60 – 3.41 (m, 3H), 3.34 (d,  $J = 3.9$  Hz, 1H), 2.83 (t,  $J = 7.7$  Hz, 2H), 2.34 – 2.21 (m, 1H), 2.14 – 2.01 (m, 3H),

1.75 – 1.65 (m, 2H), 1.47 – 1.35 (m, 2H), 0.96 (t,  $J = 7.4$  Hz, 3H);  $^{13}\text{C}$  NMR (101 MHz, DMSO- $d_6$ )  $\delta$  177.67, 167.59, 155.07, 147.60, 140.14, 129.07, 127.85, 126.21, 122.78, 55.21, 52.73, 47.88, 31.46, 30.39, 29.23, 25.01, 22.49\*, 22.09, 14.11; HRMS (ESI)  $m/z$   $[\text{M} + \text{H}]^+$  calcd. for  $\text{C}_{21}\text{H}_{29}\text{N}_8\text{O}$  409.2459, found 409.2458.

4.2.27. *(S)*-2-((3-(4-((4-(4-Methoxyphenyl)-1H-1,2,3-triazol-1-yl)methyl)phenyl)-1,2,4-oxadiazol-5-yl)methyl)pyrrolidine-1-carboximidamide hydrochloride (**21e**)

Synthesized by general procedure D: Yield: 91%; White solid;  $^1\text{H}$  NMR (400 MHz,  $\text{CD}_3\text{OD}$ )  $\delta$  8.41 (s, 1H), 8.10 (d,  $J = 8.1$  Hz, 2H), 7.74 (d,  $J = 8.6$  Hz, 2H), 7.54 (d,  $J = 8.1$  Hz, 2H), 7.01 (d,  $J = 8.6$  Hz, 2H), 5.76 (s, 2H), 4.52 (d,  $J = 6.8$  Hz, 1H), 3.83 (s, 3H), 3.66 (d,  $J = 3.7$  Hz, 1H), 3.58 – 3.41 (m, 2H), 3.32 (d,  $J = 1.6$  Hz, 1H), 2.32 – 2.22 (m, 1H), 2.15 – 1.99 (m, 3H);  $^{13}\text{C}$  NMR (101 MHz, DMSO- $d_6$ )  $\delta$  177.69, 167.60, 159.47, 155.06, 147.06, 139.98, 129.14, 127.91, 126.96, 126.29, 123.60, 121.29, 114.74, 55.59, 55.21, 52.99, 47.87, 30.39, 29.24, 22.49; HRMS (ESI)  $m/z$   $[\text{M} + \text{H}]^+$  calcd. for  $\text{C}_{24}\text{H}_{27}\text{N}_8\text{O}_2$  459.2251, found 459.2251.

4.2.28. *(S)*-2-((3-(4-((4-Cyclopropyl-1H-1,2,3-triazol-1-yl)methyl)phenyl)-1,2,4-oxadiazol-5-yl)methyl)pyrrolidine-1-carboximidamide hydrochloride (**21f**)

Synthesized by general procedure D: Yield: 75%; White solid;  $^1\text{H}$  NMR (400 MHz,  $\text{CD}_3\text{OD}$ )  $\delta$  8.29 (s, 1H), 8.11 (d,  $J = 8.0$  Hz, 2H), 7.57 (d,  $J = 8.1$  Hz, 2H), 5.79 (s, 2H), 4.58 – 4.51 (m, 1H), 3.76 – 3.63 (m, 1H), 3.63 – 3.43 (m, 3H), 2.34 – 2.23 (m, 1H), 2.17 – 2.01 (m, 4H), 1.18 – 1.13 (m, 2H), 0.92 (q,  $J = 5.2$  Hz, 2H);  $^{13}\text{C}$  NMR (101 MHz, DMSO- $d_6$ )  $\delta$  177.68, 167.59, 155.07, 149.69, 140.09, 129.07, 127.85, 126.21, 121.63, 55.21, 52.75, 47.88, 30.39, 29.24, 22.49, 8.12, 6.93; HRMS (ESI)  $m/z$   $[\text{M} + \text{H}]^+$  calcd. for  $\text{C}_{20}\text{H}_{25}\text{N}_8\text{O}$  393.2146, found 393.2141.

4.2.29. *(S)*-2-((3-(4-((4-(1-Methyl-1H-pyrazol-4-yl)-1H-1,2,3-triazol-1-yl)methyl)phenyl)-1,2,4-oxadiazol-5-yl)methyl)pyrrolidine-1-carboximidamide hydrochloride (**21g**)

Synthesized by general procedure D: Yield: 71%; White solid;  $^1\text{H}$  NMR (400 MHz,  $\text{CD}_3\text{OD}$ )  $\delta$  8.50 (d,  $J = 1.6$  Hz, 1H), 8.34 (d,  $J = 2.3$  Hz, 2H), 8.20 (s, 1H), 8.11 (d,  $J = 8.1$  Hz, 2H), 8.04 (s, 1H), 7.58 (d,  $J = 8.1$  Hz, 2H), 6.86 (s, 1H), 5.81 (s, 2H), 4.53 (q,  $J = 8.1$  Hz, 1H), 4.01 (s, 3H), 3.66 (s, 1H), 3.59 – 3.41 (m, 2H), 3.34 (d,  $J = 5.3$  Hz, 1H), 2.33 – 2.24 (dt,  $J = 18.3, 7.3$  Hz, 1H), 2.17 – 1.98 (m, 3H);  $^{13}\text{C}$  NMR (101 MHz,  $\text{CD}_3\text{OD} + \text{DMSO-d}_6$ )  $\delta$  177.50, 167.58, 154.68, 140.72, 139.79, 136.48, 133.77, 128.98, 128.32, 127.79, 126.36, 120.68, 112.88, 106.25, 55.31, 52.85, 47.79, 38.68, 30.33, 29.05, 22.38; HRMS (ESI)  $m/z$   $[\text{M} + \text{H}]^+$  calcd. for  $\text{C}_{21}\text{H}_{25}\text{N}_{10}\text{O}$  433.2207, found 433.2203.

4.2.30. *(S)*-tert-Butyl-2-((3-(4-(azidomethyl)phenyl)-1,2,4-oxadiazol-5-yl)pyrrolidine-1-carboxylate (**22**)

Synthesized by general procedure A: Yield: 89%; Liquid;  $^1\text{H}$  NMR (400 MHz,  $\text{CDCl}_3$ )  $\delta$  8.08 (d,  $J = 7.8$  Hz, 2H), 7.42 (d,  $J = 7.9$  Hz, 2H), 5.21 – 5.03 (m, 1H), 4.40 (s, 2H), 3.75 – 3.61 (m, 1H), 3.58 – 3.47 (m, 1H), 2.44 – 2.29 (m, 1H), 2.16 – 2.09 (m, 2H), 2.01 – 1.94 (m, 1H), 1.44 (s, 3H), 1.28 (s, 6H).

4.2.31. *(S)*-tert-Butyl-2-((3-(4-((4-phenyl-1H-1,2,3-triazol-1-yl)methyl)phenyl)-1,2,4-oxadiazol-5-yl)pyrrolidine-1-carboxylate (**23a**)

Synthesized by general procedure B: Yield: 78%; White solid;  $^1\text{H}$  NMR (400 MHz,  $\text{CDCl}_3$ )  $\delta$  8.08 (d,  $J = 7.9$  Hz, 2H), 7.79 (d,  $J = 7.7$  Hz, 2H), 7.69 (d,  $J = 8.7$  Hz, 1H), 7.39 (t,  $J = 7.6$  Hz, 4H), 7.30 (t,  $J = 7.3$  Hz, 1H), 5.62 (s, 2H), 5.21 – 5.02 (m, 1H), 3.72 – 3.63 (m, 1H), 3.57 – 3.44 (m, 1H), 2.42 – 2.33 (m, 1H), 2.19 – 2.06 (m, 2H), 2.00 – 1.95 (m, 1H), 1.44 (s, 3H), 1.27 (s, 6H).

4.2.32. *(S)*-tert-Butyl-2-((3-(4-((4-(4-(trifluoromethyl)phenyl)-1*H*-1,2,3-triazol-1-yl)methyl)phenyl)-1,2,4-oxadiazol-5-yl)pyrrolidine-1-carboxylate (**23b**)

Synthesized by general procedure B: Yield: 83%; White solid;  $^1\text{H}$  NMR (400 MHz,  $\text{CDCl}_3$ )  $\delta$  8.03 (d,  $J = 7.4$  Hz, 2H), 7.85 (d,  $J = 7.9$  Hz, 2H), 7.74 (s, 1H), 7.58 (d,  $J = 7.4$  Hz, 2H), 7.34 (dd,  $J = 14.0$ , 7.9 Hz, 2H), 5.58 (s, 2H), 5.13 – 4.98 (m, 1H), 3.68 – 3.55 (m, 1H), 3.49 – 3.41 (m, 1H), 2.40 – 2.25 (m, 1H), 2.13 – 1.99 (m, 2H), 1.96 – 1.91 (m, 1H), 1.38 (s, 4H), 1.21 (s, 5H).

4.2.33. *(S)*-tert-Butyl-2-((3-(4-((4-(pyridin-2-yl)-1*H*-1,2,3-triazol-1-yl)methyl)phenyl)-1,2,4-oxadiazol-5-yl)pyrrolidine-1-carboxylate (**23c**)

Synthesized by general procedure B: Yield: 80%; White solid;  $^1\text{H}$  NMR (400 MHz,  $\text{CDCl}_3$ )  $\delta$  8.52 (d,  $J = 4.8$  Hz, 1H), 8.16 (d,  $J = 7.8$  Hz, 1H), 8.08 (d,  $J = 5.2$  Hz, 2H), 7.83 – 7.71 (m, 1H), 7.42 (d,  $J = 8.1$  Hz, 2H), 7.20 (dd,  $J = 6.9$ , 5.4 Hz, 1H), 5.63 (s, 2H), 5.21 – 5.00 (m, 1H), 3.77 – 3.62 (m, 1H), 3.60 – 3.43 (m, 1H), 2.45 – 2.30 (m, 1H), 2.19 – 2.08 (m, 2H), 2.01 – 1.94 (m, 1H), 1.44 (s, 3H), 1.26 (s, 6H).

4.2.34. *(S)*-tert-Butyl-2-((3-(4-((4-(4-methoxyphenyl)-1*H*-1,2,3-triazol-1-yl)methyl)phenyl)-1,2,4-oxadiazol-5-yl)pyrrolidine-1-carboxylate (**23d**)

Synthesized by general procedure B: Yield: 81%; White solid;  $^1\text{H}$  NMR (400 MHz,  $\text{CDCl}_3$ )  $\delta$  8.07 (d,  $J = 8.0$  Hz, 2H), 7.71 (d,  $J = 8.8$  Hz, 2H), 7.60 (d,  $J = 8.6$  Hz, 1H), 7.38 (t,  $J = 9.9$  Hz, 2H), 6.92 (d,  $J = 8.7$  Hz, 2H), 5.60 (s, 2H), 5.21 – 5.00 (m, 1H), 3.81 (s, 3H), 3.73 – 3.45 (m, 2H), 2.44 – 2.30 (m, 1H), 2.19 – 2.06 (m, 2H), 2.01 – 1.94 (m, 1H), 1.44 (s, 3H), 1.26 (s, 6H).

4.2.35. *(S)*-tert-Butyl-2-((3-(4-((4-(thiophen-2-yl)-1*H*-1,2,3-triazol-1-yl)methyl)phenyl)-1,2,4-oxadiazol-5-yl)-pyrrolidine-1-carboxylate (**23e**)

Synthesized by general procedure B: Yield: 74%; Brown solid;  $^1\text{H}$  NMR (400 MHz,  $\text{CDCl}_3$ )  $\delta$  8.08 (d,  $J = 7.7$  Hz, 2H), 7.59 (d,  $J = 7.8$  Hz, 1H), 7.37 (dd,  $J = 22.6$ , 5.6 Hz, 3H), 7.27 (d,  $J = 5.2$  Hz, 1H),

7.08 – 7.01 (m, 1H), 5.60 (s, 2H), 5.21 – 5.01 (m, 1H), 3.76 – 3.42 (m, 2H), 2.44 – 2.34 (m, 1H), 2.15 – 1.97 (m, 3H), 1.44 (s, 3H), 1.27 (s, 6H).

4.2.36. (*S*)-*tert*-Butyl-2-((3-(4-((4-butyl-1*H*-1,2,3-triazol-1-yl)methyl)phenyl)-1,2,4-oxadiazol-5-yl)-pyrrolidine-1-carboxylate (**23f**)

Synthesized by general procedure B: Yield: 85%; White solid;  $^1\text{H}$  NMR (400 MHz,  $\text{CDCl}_3$ )  $\delta$  8.05 (d,  $J = 8.0$  Hz, 2H), 7.32 (t,  $J = 8.8$  Hz, 2H), 7.19 (d,  $J = 10.0$  Hz, 1H), 5.53 (s, 2H), 5.21 – 5.03 (m, 1H), 3.72 – 3.60 (m, 1H), 3.57 – 3.44 (m, 1H), 2.68 (t,  $J = 7.7$  Hz, 2H), 2.42 – 2.31 (m, 1H), 2.18 – 2.08 (m, 2H), 2.01 – 1.95 (m, 1H), 1.65 – 1.58 (m, 2H), 1.44 (s, 3H), 1.34 (dd,  $J = 14.9, 7.5$  Hz, 2H), 1.27 (s, 6H), 0.89 (t,  $J = 7.3$  Hz, 3H).

4.2.37. (*S*)-*tert*-Butyl-2-((3-(4-((4-(4-(fluorophenyl)-1*H*-1,2,3-triazol-1-yl)methyl)phenyl)-1,2,4-oxadiazol-5-yl)pyrrolidine-1-carboxylate (**23g**)

Synthesized by general procedure B: Yield: 56%; White solid;  $^1\text{H}$  NMR (400 MHz,  $\text{CDCl}_3$ )  $\delta$  8.08 (d,  $J = 7.7$  Hz, 2H), 7.76 (dd,  $J = 8.1, 5.5$  Hz, 2H), 7.64 (d,  $J = 9.4$  Hz, 1H), 7.38 (t,  $J = 10.1$  Hz, 2H), 7.07 (t,  $J = 8.6$  Hz, 2H), 5.61 (s, 2H), 5.19 – 5.03 (m, 1H), 3.72 – 3.44 (m, 2H), 2.40 – 2.34 (m, 1H), 2.17 – 2.08 (m, 2H), 1.99 – 1.95 (m, 1H), 1.43 (s, 3H), 1.26 (s, 6H).

4.2.38. (*S*)-*tert*-Butyl-2-((3-(4-((4-cyclopropyl-1*H*-1,2,3-triazol-1-yl)methyl)phenyl)-1,2,4-oxadiazol-5-yl)pyrrolidine-1-carboxylate (**23h**)

Synthesized by general procedure B: Yield: 85%; White solid;  $^1\text{H}$  NMR (400 MHz,  $\text{CDCl}_3$ )  $\delta$  8.05 (d,  $J = 7.9$  Hz, 2H), 7.31 (t,  $J = 10.5$  Hz, 2H), 7.16 (t,  $J = 7.5$  Hz, 1H), 5.50 (s, 2H), 5.18 – 5.03 (m, 1H), 3.74 – 3.60 (m, 1H), 3.55 – 3.45 (m, 1H), 2.39 – 2.34 (m, 1H), 2.15 – 2.08 (m, 2H), 1.99 – 1.97 (m, 1H), 1.94 – 1.87 (m, 1H), 1.43 (s, 3H), 1.25 (s, 6H), 0.95 – 0.87 (m, 2H), 0.81 (d,  $J = 3.9$  Hz, 2H).

4.2.39. *(S)*-*tert*-Butyl-(((*tert*-butoxycarbonyl)imino)(2-((3-(4-((4-phenyl-1*H*-1,2,3-triazol-1-yl)methyl)phenyl)-1,2,4-oxadiazol-5-yl)pyrrolidin-1-yl)methyl)carbamate (**24a**)

Synthesized by general procedure C: Yield: 47%; White solid;  $^1\text{H}$  NMR (400 MHz,  $\text{CDCl}_3$ )  $\delta$  10.09 (s, 1H), 8.08 (d,  $J = 8.3$  Hz, 2H), 7.79 (d,  $J = 7.1$  Hz, 2H), 7.68 (s, 1H), 7.42 – 7.36 (m, 4H), 7.32 – 7.28 (m, 1H), 5.63 (s, 2H), 5.59 (dd,  $J = 7.8, 4.5$  Hz, 1H), 3.92 – 3.83 (m, 1H), 3.82 – 3.72 (m, 1H), 2.46 – 2.38 (m, 1H), 2.21 – 2.13 (m, 2H), 1.62 (s, 1H), 1.46 (s, 9H), 1.39 (s, 9H).

4.2.40. *(S)*-*tert*-Butyl-(((*tert*-butoxycarbonyl)imino)(2-((3-(4-((4-(4-(trifluoromethyl)phenyl)-1*H*-1,2,3-triazol-1-yl)methyl)phenyl)-1,2,4-oxadiazol-5-yl)pyrrolidin-1-yl)methyl)carbamate (**24b**)

Synthesized by general procedure C: Yield: 32%; White solid;  $^1\text{H}$  NMR (400 MHz,  $\text{CDCl}_3$ )  $\delta$  9.99 (s, 1H), 7.99 (d,  $J = 8.1$  Hz, 2H), 7.80 (d,  $J = 8.1$  Hz, 2H), 7.65 (s, 1H), 7.54 (d,  $J = 8.2$  Hz, 2H), 7.30 (d,  $J = 8.1$  Hz, 2H), 5.54 (s, 2H), 5.49 (dd,  $J = 7.7, 4.4$  Hz, 1H), 3.81 – 3.62 (m, 2H), 2.38 – 2.27 (m, 1H), 2.11 – 2.03 (m, 2H), 1.92 – 1.87 (m, 1H), 1.37 – 1.29 (m, 18H).

4.2.41. *(S)*-*tert*-Butyl-(((*tert*-butoxycarbonyl)imino)(2-((3-(4-((4-(pyridin-2-yl)-1*H*-1,2,3-triazol-1-yl)methyl)phenyl)-1,2,4-oxadiazol-5-yl)pyrrolidin-1-yl)methyl)carbamate (**24c**)

Synthesized by general procedure C: Yield: 25%; White solid;  $^1\text{H}$  NMR (400 MHz,  $\text{CDCl}_3$ )  $\delta$  10.11 (s, 1H), 8.52 (d,  $J = 4.8$  Hz, 1H), 8.16 (d,  $J = 8.0$  Hz, 1H), 8.07 (d,  $J = 8.4$  Hz, 3H), 7.75 (td,  $J = 7.7, 1.4$  Hz, 1H), 7.40 (d,  $J = 8.1$  Hz, 2H), 7.20 (dd,  $J = 6.9, 5.5$  Hz, 1H), 5.63 (s, 2H), 5.58 (dd,  $J = 7.7, 4.5$  Hz, 1H), 3.90 – 3.84 (m, 1H), 3.80 – 3.72 (m, 1H), 2.48 – 2.36 (m, 1H), 2.21 – 2.13 (m, 2H), 1.72 (br s, 1H), 1.46 (s, 9H), 1.39 (s, 9H).

4.2.42. (*S*)-*tert*-Butyl-(((*tert*-butoxycarbonyl)imino)(2-((3-(4-((4-(4-methoxyphenyl)-1*H*-1,2,3-triazol-1-yl)methyl)phenyl)-1,2,4-oxadiazol-5-yl)pyrrolidin-1-yl)methyl)carbamate (**24d**)

Synthesized by general procedure C: Yield: 33%; White solid;  $^1\text{H}$  NMR (400 MHz,  $\text{CDCl}_3$ )  $\delta$  10.08 (s, 1H), 8.07 (d,  $J = 8.2$  Hz, 2H), 7.71 (d,  $J = 8.8$  Hz, 2H), 7.59 (s, 1H), 7.37 (d,  $J = 8.3$  Hz, 2H), 6.91 (d,  $J = 8.8$  Hz, 2H), 5.60 (s, 2H), 5.59 – 5.56 (m, 1H), 3.91 – 3.83 (m, 1H), 3.81 (s, 3H), 3.79 – 3.72 (m, 1H), 2.48 – 2.38 (m, 1H), 2.20 – 2.13 (m, 2H), 1.66 (s, 1H), 1.46 (s, 9H), 1.39 (s, 9H).

4.2.43. (*S*)-*tert*-Butyl-(((*tert*-butoxycarbonyl)imino)(2-((3-(4-((4-(thiophen-2-yl)-1*H*-1,2,3-triazol-1-yl)methyl)phenyl)-1,2,4-oxadiazol-5-yl)pyrrolidin-1-yl)methyl)carbamate (**24e**)

Synthesized by general procedure C: Yield: 19%; Brown solid;  $^1\text{H}$  NMR (400 MHz,  $\text{CDCl}_3$ )  $\delta$  10.08 (s, 1H), 8.08 (d,  $J = 8.2$  Hz, 2H), 7.59 (s, 1H), 7.38 (d,  $J = 8.2$  Hz, 2H), 7.33 (d,  $J = 4.6$  Hz, 1H), 7.27 (d,  $J = 5.1$  Hz, 1H), 7.06 – 7.01 (m, 1H), 5.62 – 5.56 (m, 3H), 3.90 – 3.84 (m, 1H), 3.83 – 3.72 (m, 1H), 2.49 – 2.37 (m, 1H), 2.17 – 2.13 (m, 2H), 2.01 – 1.99 (m, 1H), 1.44 (br m, 18H).

4.2.44. (*S*)-*tert*-Butyl-(((*tert*-butoxycarbonyl)imino)(2-((3-(4-((4-butyl-1*H*-1,2,3-triazol-1-yl)methyl)phenyl)-1,2,4-oxadiazol-5-yl)pyrrolidin-1-yl)methyl)carbamate (**24f**)

Synthesized by general procedure C: Yield: 19%; White solid;  $^1\text{H}$  NMR (400 MHz,  $\text{CDCl}_3$ )  $\delta$  10.09 (s, 1H), 8.05 (d,  $J = 8.2$  Hz, 2H), 7.32 (d,  $J = 8.1$  Hz, 2H), 7.24 (s, 1H), 5.58 (dd,  $J = 7.6, 4.5$  Hz, 1H), 5.53 (s, 2H), 3.90 – 3.84 (m, 1H), 3.82 – 3.74 (m, 1H), 2.69 (t,  $J = 7.7$  Hz, 2H), 2.48 – 2.38 (m, 1H), 2.21 – 2.17 (m, 2H), 2.02 – 1.97 (m, 1H), 1.65 – 1.57 (m, 2H), 1.46 (s, 9H), 1.40 (s, 9H), 1.24 (t,  $J = 6.6$  Hz, 2H), 0.89 (t,  $J = 7.3$  Hz, 3H).

4.2.45. *(S)*-*tert*-Butyl-(((*tert*-butoxycarbonyl)imino)(2-((3-(4-((4-(4-fluorophenyl)-1*H*-1,2,3-triazol-1-yl)methyl)phenyl)-1,2,4-oxadiazol-5-yl)pyrrolidin-1-yl)methyl)carbamate (**24g**)

Synthesized by general procedure C: Yield: 35%; White solid;  $^1\text{H}$  NMR (400 MHz,  $\text{CDCl}_3$ )  $\delta$  10.09 (s, 1H), 8.08 (d,  $J = 8.2$  Hz, 2H), 7.76 (dd,  $J = 8.2, 5.9$  Hz, 2H), 7.63 (s, 1H), 7.38 (d,  $J = 8.0$  Hz, 2H), 7.07 (t,  $J = 8.7$  Hz, 2H), 5.62 (s, 2H), 5.59 (dd,  $J = 7.8, 4.4$  Hz, 1H), 3.90 – 3.75 (m, 2H), 2.46 – 2.40 (m, 1H), 2.22 – 2.13 (m, 2H), 2.02 – 1.97 (m, 1H), 1.46 (s, 9H), 1.39 (s, 9H).

4.2.46. *(S)*-*tert*-Butyl-(((*tert*-butoxycarbonyl)imino)(2-((3-(4-((4-cyclopropyl)-1*H*-1,2,3-triazol-1-yl)methyl)phenyl)-1,2,4-oxadiazol-5-yl)pyrrolidin-1-yl)methyl)carbamate (**24h**)

Synthesized by general procedure C: Yield: 16%; White solid;  $^1\text{H}$  NMR (400 MHz,  $\text{CDCl}_3$ )  $\delta$  10.08 (s, 1H), 8.04 (d,  $J = 8.1$  Hz, 2H), 7.31 (d,  $J = 8.0$  Hz, 2H), 7.14 (s, 1H), 5.58 (dd,  $J = 7.6, 4.4$  Hz, 1H), 5.50 (s, 2H), 3.92 – 3.72 (m, 2H), 2.50 – 2.38 (m, 1H), 2.19 – 2.13 (m, 2H), 2.00 – 1.87 (m, 1H), 1.72 (br s, 1H), 1.46 (s, 9H), 1.39 (s, 9H), 0.93 – 0.88 (m, 2H), 0.83 – 0.79 (m, 2H).

4.2.47. *(S)*-2-((3-(4-((4-Phenyl)-1*H*-1,2,3-triazol-1-yl)methyl)phenyl)-1,2,4-oxadiazol-5-yl)pyrrolidine-1-carboximidamide hydrochloride (**25a**)

Synthesized by general procedure D: Yield: 81%; White solid;  $^1\text{H}$  NMR (400 MHz,  $\text{CD}_3\text{OD}$ )  $\delta$  8.57 (s, 1H), 8.12 (dd,  $J = 19.3, 8.1$  Hz, 2H), 7.82 (d,  $J = 7.7$  Hz, 2H), 7.57 (t,  $J = 7.8$  Hz, 2H), 7.46 (t,  $J = 7.6$  Hz, 2H), 7.38 (t,  $J = 7.3$  Hz, 1H), 5.80 (d,  $J = 4.2$  Hz, 2H), 5.48 – 5.18 (m, 1H), 3.78 – 3.53 (m, 2H), 2.72 – 2.52 (m, 1H), 2.47 – 2.37 (m, 1H), 2.32 – 2.20 (m, 1H), 2.15 – 2.02 (m, 1H);  $^{13}\text{C}$  NMR (101 MHz,  $\text{DMSO-d}_6$ )  $\delta$  178.77, 175.79, 167.72, 167.70, 155.90, 147.11, 140.24, 140.03\*, 131.01, 129.33, 129.21, 128.37, 128.01, 126.00\*, 125.76\*, 125.60, 122.33, 122.28\*, 55.18, 53.19, 53.01\*, 48.10\*, 45.75, 31.81\*, 29.09, 23.72, 23.27\*; HRMS (ESI)  $m/z$   $[\text{M} + \text{H}]^+$  calcd. for  $\text{C}_{22}\text{H}_{23}\text{N}_8\text{O}$  415.1989, found 415.1987.

4.2.48. (*S*)-2-((3-(4-((4-(4-(Trifluoromethyl)phenyl)-1*H*-1,2,3-triazol-1-yl)methyl)phenyl)-1,2,4-oxadiazol-5-yl)pyrrolidine-1-carboximidamide hydrochloride (**25b**)

Synthesized by general procedure D: Yield: 78%; White solid;  $^1\text{H}$  NMR (400 MHz,  $\text{CD}_3\text{OD}$ )  $\delta$  8.54 (d,  $J = 10.7$  Hz, 1H), 8.09 (d,  $J = 8.1$  Hz, 1H), 8.02 (d,  $J = 8.1$  Hz, 2H), 7.97 (d,  $J = 8.2$  Hz, 1H), 7.73 (d,  $J = 8.2$  Hz, 2H), 7.54 (d,  $J = 8.1$  Hz, 1H), 7.48 (d,  $J = 8.2$  Hz, 1H), 5.75 (d,  $J = 10.5$  Hz, 2H), 5.44 (d,  $J = 7.7$  Hz, 1H), 3.76 (td,  $J = 9.2, 2.3$  Hz, 1H), 3.61 (dt,  $J = 17.2, 8.7$  Hz, 1H), 2.61 – 2.41 (m, 2H), 2.29 – 2.17 (m, 1H), 2.16 – 2.01 (m, 1H);  $^{13}\text{C}$  NMR (101 MHz,  $\text{DMSO-d}_6$ )  $\delta$  178.76, 171.95, 167.76\*, 167.69, 155.81, 145.73, 139.82, 138.92\*, 134.99, 129.30, 128.90, 128.03, 127.71, 127.60, 126.34, 126.31, 126.14, 126.08\*, 123.55, 123.48\*, 55.20, 53.23\*, 53.15, 48.10, 31.82, 23.28; HRMS (ESI)  $m/z$   $[\text{M} + \text{H}]^+$  calcd. for  $\text{C}_{23}\text{H}_{22}\text{F}_3\text{N}_8\text{O}$  483.1863, found 483.1857.

4.2.49. (*S*)-2-(3-(4-((4-(Pyridin-2-yl)-1*H*-1,2,3-triazol-1-yl)methyl)phenyl)-1,2,4-oxadiazol-5-yl)pyrrolidine-1-carboximidamide hydrochloride (**25c**)

Synthesized by general procedure D: Yield: 71%; White solid;  $^1\text{H}$  NMR (400 MHz,  $\text{CD}_3\text{OD}$ )  $\delta$  9.04 (s, 1H), 8.77 (d,  $J = 5.7$  Hz, 1H), 8.62 (t,  $J = 8.1$  Hz, 1H), 8.45 (d,  $J = 8.1$  Hz, 1H), 8.17 – 8.08 (m, 2H), 7.96 (t,  $J = 6.7$  Hz, 1H), 7.60 (d,  $J = 8.2$  Hz, 2H), 5.87 (s, 2H), 5.45 (dd,  $J = 8.0, 1.1$  Hz, 1H), 3.76 (td,  $J = 9.2, 2.0$  Hz, 1H), 3.65 – 3.58 (m, 1H), 2.61 – 2.42 (m, 2H), 2.31 – 2.20 (m, 1H), 2.13 – 2.01 (m, 1H);  $^{13}\text{C}$  NMR (101 MHz,  $\text{DMSO-d}_6$ )  $\delta$  178.79, 175.74\*, 167.64, 155.92, 145.47\*, 144.98, 143.88, 142.57\*, 139.41, 129.44, 128.04, 126.48, 126.18, 125.31, 122.63, 55.20, 53.36, 53.17\*, 48.13, 45.73\*, 31.80, 29.09\*, 23.74\*, 23.27; HRMS (ESI)  $m/z$   $[\text{M} + \text{H}]^+$  calcd. for  $\text{C}_{21}\text{H}_{22}\text{N}_9\text{O}$  416.1942, found 416.1941.

4.2.50. (*S*)-2-((3-(4-((4-(4-Methoxyphenyl)-1*H*-1,2,3-triazol-1-yl)methyl)phenyl)-1,2,4-oxadiazol-5-yl)pyrrolidine-1-carboximidamide hydrochloride (**25d**)

Synthesized by general procedure D: Yield: 89%; White solid;  $^1\text{H}$  NMR (400 MHz,  $\text{CD}_3\text{OD}$ )  $\delta$  8.61 (s, 1H), 8.11 (dd,  $J = 18.9, 8.2$  Hz, 2H), 7.75 (d,  $J = 8.7$  Hz, 2H), 7.59 (d,  $J = 8.1$  Hz, 2H), 7.04 (d,  $J =$

8.7 Hz, 2H), 5.83 (s, 2H), 5.45 (d,  $J = 7.0$  Hz, 1H), 3.84 (s, 3H), 3.79 – 3.74 (m, 1H), 3.65 – 3.58 (m, 1H), 2.62 – 2.42 (m, 2H), 2.28 – 2.03 (m, 2H);  $^{13}\text{C}$  NMR (101 MHz, DMSO- $d_6$ )  $\delta$  178.76, 175.78\*, 167.70, 159.46, 155.89, 147.04, 140.09, 129.18, 127.99, 126.97, 125.98\*, 123.59, 121.30, 114.73, 55.59, 55.18, 53.20\*, 52.98, 48.10, 45.76\*, 31.81, 29.09\*, 23.72\*, 23.27; HRMS (ESI)  $m/z$   $[\text{M} + \text{H}]^+$  calcd. for  $\text{C}_{23}\text{H}_{25}\text{N}_8\text{O}_2$  445.2095, found 445.2092.

4.2.51. (*S*)-2-((3-(4-((4-(Thiophen-2-yl)-1*H*-1,2,3-triazol-1-yl)methyl)phenyl)-1,2,4-oxadiazol-5-yl)-pyrrolidine-1-carboximidamide hydrochloride (**25e**)

Synthesized by general procedure D: Yield: 51%; Brown solid;  $^1\text{H}$  NMR (400 MHz,  $\text{CD}_3\text{OD}$ )  $\delta$  8.35 – 8.29 (m, 2H), 8.09 (d,  $J = 8.1$  Hz, 1H), 7.56 – 7.49 (m, 2H), 7.42 (d,  $J = 4.2$  Hz, 2H), 7.11 – 7.07 (m, 1H), 5.72 (s, 2H), 5.45 (d,  $J = 7.9$  Hz, 1H), 3.80 – 3.72 (m, 1H), 3.66 – 3.57 (m, 1H), 2.61 – 2.41 (m, 2H), 2.31 – 2.18 (m, 1H), 2.15 – 2.03 (m, 1H);  $^{13}\text{C}$  NMR (101 MHz, DMSO- $d_6$ )  $\delta$  178.76, 167.70, 155.83, 142.50, 139.89, 133.68\*, 133.25, 129.24, 128.33, 128.02, 126.04\*, 125.89, 124.67, 121.52, 105.29, 55.19, 53.04, 48.10, 31.82, 31.73\*, 23.70\*, 23.28; HRMS (ESI)  $m/z$   $[\text{M} + \text{H}]^+$  calcd. for  $\text{C}_{20}\text{H}_{21}\text{N}_8\text{OS}$  421.1554, found 421.1550.

4.2.52. (*S*)-2-((3-(4-((4-Butyl-1*H*-1,2,3-triazol-1-yl)methyl)phenyl)-1,2,4-oxadiazol-5-yl)pyrrolidine-1-carboximidamide hydrochloride (**25f**)

Synthesized by general procedure D: Yield: 73%; White solid;  $^1\text{H}$  NMR (400 MHz,  $\text{CD}_3\text{OD}$ )  $\delta$  8.34 (d,  $J = 2.1$  Hz, 1H), 8.11 (d,  $J = 8.0$  Hz, 2H), 7.58 (d,  $J = 7.8$  Hz, 2H), 5.83 (s, 2H), 5.46 (d,  $J = 7.8$  Hz, 1H), 3.77 (t,  $J = 8.2$  Hz, 1H), 3.64 – 3.58 (m, 1H), 2.82 (t,  $J = 7.7$  Hz, 2H), 2.60 – 2.45 (m, 2H), 2.29 – 2.03 (m, 2H), 1.75 – 1.65 (m, 2H), 1.46 – 1.35 (m, 2H), 0.96 (t,  $J = 7.3$  Hz, 3H);  $^{13}\text{C}$  NMR (101 MHz, DMSO- $d_6$ )  $\delta$  178.74, 167.70, 155.85, 147.61, 140.31, 129.10, 127.93, 125.88, 122.74, 55.18, 52.71, 48.09, 31.81\*, 31.46, 25.02, 23.27\*, 22.08, 14.11; HRMS (ESI)  $m/z$   $[\text{M} + \text{H}]^+$  calcd. for  $\text{C}_{20}\text{H}_{27}\text{N}_8\text{O}$  395.2302, found 395.2297.

4.2.53. *(S)*-2-((3-(4-((4-(4-Fluorophenyl)-1*H*-1,2,3-triazol-1-yl)methyl)phenyl)-1,2,4-oxadiazol-5-yl)-pyrrolidine-1-carboximidamide hydrochloride (**25g**)

Synthesized by general procedure D: Yield: 79%; White solid;  $^1\text{H}$  NMR (400 MHz,  $\text{CD}_3\text{OD}$ )  $\delta$  8.49 (s, 1H), 8.34 (d,  $J = 2.6$  Hz, 1H), 8.15 – 8.07 (m, 2H), 7.85 (dd,  $J = 8.3, 5.5$  Hz, 2H), 7.55 (d,  $J = 8.1$  Hz, 2H), 7.19 (t,  $J = 8.7$  Hz, 2H), 5.77 (s, 2H), 5.45 (d,  $J = 7.6$  Hz, 1H), 3.76 (td,  $J = 9.1, 2.0$  Hz, 1H), 3.63 – 3.57 (m, 1H), 2.61 – 2.41 (m, 2H), 2.30 – 2.19 (m, 1H), 2.13 – 2.01 (m, 1H);  $^{13}\text{C}$  NMR (101 MHz, DMSO- $d_6$ )  $\delta$  178.34, 167.28, 160.58\*, 155.43, 145.83, 139.56, 133.33, 128.79, 127.59, 127.26\*, 127.18, 125.59, 121.75, 115.95, 115.74\*, 105.29, 54.77, 52.62, 47.67, 45.38\*, 31.40, 22.86; HRMS (ESI)  $m/z$   $[\text{M} + \text{H}]^+$  calcd. for  $\text{C}_{22}\text{H}_{22}\text{FN}_8\text{O}$  433.1895, found 433.1888.

4.2.54. *(S)*-2-((3-(4-((4-Cyclopropyl)-1*H*-1,2,3-triazol-1-yl)methyl)phenyl)-1,2,4-oxadiazol-5-yl)pyrrolidine-1-carboximidamide hydrochloride (**25h**)

Synthesized by general procedure D: Yield: 71%; White solid;  $^1\text{H}$  NMR (400 MHz,  $\text{CD}_3\text{OD}$ )  $\delta$  8.28 (s, 1H), 8.13 (dd,  $J = 18.9, 8.2$  Hz, 2H), 7.61 – 7.54 (m, 2H), 5.79 (s, 2H), 5.46 (d,  $J = 8.0$  Hz, 1H), 3.82 – 3.73 (m, 1H), 3.63 – 3.56 (m, 1H), 2.62 – 2.43 (m, 2H), 2.30 – 2.21 (m, 1H), 2.13 – 2.06 (m, 2H), 1.19 – 1.12 (m, 2H), 0.95 – 0.88 (m, 2H);  $^{13}\text{C}$  NMR (101 MHz, DMSO- $d_6$ )  $\delta$  178.75, 175.76\*, 167.69, 155.90, 149.64, 140.35\*, 140.16, 133.12, 129.13, 129.02\*, 127.93, 125.91, 125.67, 121.75\*, 121.70, 55.18, 53.18\*, 52.80, 48.09, 45.74\*, 31.80, 31.72\*, 23.72\*, 23.27, 8.14, 6.89; HRMS (ESI)  $m/z$   $[\text{M} + \text{H}]^+$  calcd. for  $\text{C}_{19}\text{H}_{23}\text{N}_8\text{O}$  379.1989, found 379.1996.

4.2.55. 4-(Azidomethyl)-*N'*-((1-cyanocyclopropanecarbonyl)oxy)benzimidamide (**26**)

To a suspension of 1-cyanopropanecarboxylic acid (0.29 g, 2.61 mmol), PyBOP (1.36 g, 2.61 mmol), and **17** (0.5 g, 2.61 mmol) in  $\text{CH}_2\text{Cl}_2$  (10 mL) at rt was added DIEA (1.8 mL, 10.44 mmol) and was stirred for 4 h until the reaction was completed as determined by the TLC. The reaction was then evaporated to dryness and immediately purified by silica gel column chromatography, to afford **26** (0.4

g, 54% yield) as a white solid.  $^1\text{H}$  NMR (400 MHz,  $\text{CDCl}_3$ )  $\delta$  7.71 (d,  $J = 8.1$  Hz, 2H), 7.37 (d,  $J = 8.0$  Hz, 2H), 5.28 (s, 2H), 4.38 (s, 2H), 1.81 (dd,  $J = 8.4, 4.6$  Hz, 2H), 1.69 (dd,  $J = 8.4, 4.6$  Hz, 2H).

4.2.56. *1-(3-(4-(Azidomethyl)phenyl)-1,2,4-oxadiazol-5-yl)cyclopropanecarbonitrile (27)*

To a solution of compound **26** (0.4 g, 1.40 mmol) in THF (2 mL) at rt was added a 1.0 M solution of TBAF in THF (0.4 mL, 1.40 mmol) and was stirred for 2 h until the reaction was completed as determined by the TLC. The reaction was evaporated to dryness and immediately purified by silica gel column chromatography, to afford **27** (0.25 g, 68% yield) as a white solid.  $^1\text{H}$  NMR (400 MHz,  $\text{CDCl}_3$ )  $\delta$  8.05 (d,  $J = 8.0$  Hz, 2H), 7.42 (d,  $J = 8.1$  Hz, 2H), 4.41 (s, 2H), 2.02 (s, 4H).

4.2.57. *1-(3-(4-((4-Phenyl-1H-1,2,3-triazol-1-yl)methyl)phenyl)-1,2,4-oxadiazol-5-yl)cyclopropanecarbonitrile (28a)*

Synthesized by general procedure B: Yield: 62%; White solid;  $^1\text{H}$  NMR (400 MHz,  $\text{DMSO-d}_6$ )  $\delta$  8.69 (s, 1H), 8.00 (d,  $J = 8.2$  Hz, 2H), 7.86 (d,  $J = 7.8$  Hz, 2H), 7.52 (d,  $J = 8.2$  Hz, 2H), 7.45 (t,  $J = 7.6$  Hz, 2H), 7.33 (t,  $J = 7.4$  Hz, 1H), 5.76 (s, 2H), 2.20 (dd,  $J = 8.8, 5.0$  Hz, 2H), 2.02 (dd,  $J = 8.8, 5.0$  Hz, 2H).

4.2.58. *1-(3-(4-((4-(1-Methyl-1H-pyrazol-5-yl)-1H-1,2,3-triazol-1-yl)methyl)phenyl)-1,2,4-oxadiazol-5-yl)cyclo-propanecarbonitrile (28b)*

Synthesized by general procedure B: Yield: 72%; White solid;  $^1\text{H}$  NMR (400 MHz,  $\text{CDCl}_3$ )  $\delta$  8.03 (d,  $J = 8.3$  Hz, 2H), 7.76 (s, 1H), 7.68 (s, 1H), 7.49 (s, 1H), 7.36 (d,  $J = 8.2$  Hz, 2H), 5.58 (s, 2H), 3.91 (s, 3H), 2.01 (s, 4H).

4.2.59. *1-(3-(4-((4-Cyclopropyl-1H-1,2,3-triazol-1-yl)methyl)phenyl)-1,2,4-oxadiazol-5-yl)cyclopropanecarbonitrile (28c)*

Synthesized by general procedure B: Yield: 85%; White solid;  $^1\text{H}$  NMR (400 MHz,  $\text{CDCl}_3$ )  $\delta$  8.01 (d,  $J = 8.1$  Hz, 2H), 7.31 (d,  $J = 8.1$  Hz, 2H), 7.17 (s, 1H), 5.50 (s, 2H), 2.05 – 1.96 (m, 4H), 1.95 – 1.86 (m, 1H), 0.95 – 0.87 (m, 2H), 0.86 – 0.77 (m, 2H).

4.2.60. *1-(3-(4-((4-Phenyl-1H-1,2,3-triazol-1-yl)methyl)phenyl)-1,2,4-oxadiazol-5-yl)cyclopropanecarboximidamide hydrochloride (29a)*

Synthesized by general procedure E: Yield: 51%; White solid;  $^1\text{H}$  NMR (400 MHz,  $\text{CD}_3\text{OD}$ )  $\delta$  8.43 (s, 1H), 8.08 (d,  $J = 8.1$  Hz, 2H), 7.82 (d,  $J = 7.7$  Hz, 2H), 7.53 (d,  $J = 7.9$  Hz, 2H), 7.43 (t,  $J = 7.3$  Hz, 2H), 7.34 (t,  $J = 7.4$  Hz, 1H), 5.75 (s, 2H), 2.02 – 1.91 (m, 4H);  $^{13}\text{C}$  NMR (101 MHz,  $\text{DMSO-d}_6$ )  $\delta$  177.93, 167.80, 166.15, 147.04, 140.12, 130.98, 129.33, 129.19, 128.37, 127.97, 125.81\*, 125.57, 122.37, 52.97, 22.50, 18.88; HRMS (ESI)  $m/z$   $[\text{M} + \text{H}]^+$  calcd. for  $\text{C}_{21}\text{H}_{20}\text{N}_7\text{O}$  386.1724, found 386.1722.

4.2.61. *1-(3-(4-((4-(1-Methyl-1H-pyrazol-5-yl)-1H-1,2,3-triazol-1-yl)methyl)phenyl)-1,2,4-oxadiazol-5-yl)cyclo-propanecarboximidamide hydrochloride (29b)*

Synthesized by general procedure E: Yield: 59%; White solid;  $^1\text{H}$  NMR (400 MHz,  $\text{CD}_3\text{OD}$ )  $\delta$  8.15 (d,  $J = 4.8$  Hz, 1H), 8.05 (t,  $J = 8.2$  Hz, 2H), 7.94 (d,  $J = 2.6$  Hz, 1H), 7.79 (s, 1H), 7.49 (dd,  $J = 7.9, 6.0$  Hz, 2H), 5.69 (d,  $J = 2.9$  Hz, 2H), 3.91 (s, 3H), 2.11 – 1.93 (m, 4H);  $^{13}\text{C}$  NMR (101 MHz,  $\text{DMSO-d}_6$ )  $\delta$  177.96, 167.85, 166.01, 140.80, 140.25, 136.63, 129.17, 129.13\*, 128.40, 128.00\*, 127.97, 125.78, 125.69\*, 120.84, 112.96, 52.82, 39.02, 22.60, 21.11, 18.73; HRMS (ESI)  $m/z$   $[\text{M} + \text{H}]^+$  calcd. for  $\text{C}_{19}\text{H}_{20}\text{N}_9\text{O}$  390.1785, found 390.1778.

4.2.62. 1-(3-(4-((4-Cyclopropyl-1H-1,2,3-triazol-1-yl)methyl)phenyl)-1,2,4-oxadiazol-5-yl)cyclopropanecarboximidamide hydrochloride (**29c**)

Synthesized by general procedure E: Yield: 55%; White solid;  $^1\text{H}$  NMR (400 MHz, DMSO- $d_6$  +  $\text{CDCl}_3$ )  $\delta$  8.05 – 7.80 (m, 5H), 5.60 (d,  $J$  = 16.3 Hz, 2H), 2.04 – 1.81 (m, 4H), 1.16 (t,  $J$  = 7.1 Hz, 1H), 0.88 (d,  $J$  = 6.0 Hz, 2H), 0.72 – 0.63 (br m, 2H);  $^{13}\text{C}$  NMR (101 MHz, DMSO- $d_6$ )  $\delta$  177.93, 167.83, 166.14, 149.70, 140.36, 129.09, 127.91, 121.62, 52.67, 22.52, 21.21\*, 18.83, 14.52, 8.10, 6.95; HRMS (ESI)  $m/z$   $[\text{M} + \text{H}]^+$  calcd. for  $\text{C}_{18}\text{H}_{20}\text{N}_7\text{O}$  350.1724, found 350.1723.

### 4.3. Biological evaluations

#### 4.3.1. Protein sequence alignment analysis

Protein sequence alignment analysis was performed using Clustal Omega multiple sequence alignment tool [54]. Proteins sequences of human SphK1 protein (UniProtKB: Q9NYA1) and human SphK2 protein (UniProtKB: Q9NRA0) were used and compared.

#### 4.3.2. *In vitro* sphingosine kinase assay

ADP-Glo (Promega, Madison, WI) kinase assay were used to evaluate the kinase activity of SphK. ATP to ADP standard curves were prepared in the kinase buffer to assess the linearity of the assay in order to calculate the amount of ADP produced in each tested conditions (**Fig. 4A**). SB10 (tenfold signal to background ratio) of SphK was also determined to evaluate the enzyme performance and to optimize the kinase reaction condition in our system. In brief, for SphK2, 100  $\mu\text{M}$  of ATP, 100  $\mu\text{M}$  of D-erythro-Sphingosine (Tocris Bioscience, Minneapolis, MN), and 2 ng of recombinant human SphK2 (R&D Systems, Minneapolis, MN) with desired concentration of each synthesized compound were used for SphK2 kinase reaction. For SphK1, exact same reaction condition was used except 0.5 ng of recombinant human SphK1 was used.

To evaluate the SphK selectivity of each compound, 125  $\mu\text{M}$  of each compound in reaction buffer (40 mM Tris, pH 8.0, 20 mM  $\text{MgCl}_2$ , and 0.1mg/mL BSA) with 5% DMSO was incubated with either SphK1 or SphK2 in a 384-well solid white low volume microplate (Corning, Corning, NY), and the reaction was initiated by adding mixture of ATP and D-erythro-Sphingosine to a total volume of 5  $\mu\text{L}$ , after 1 hour incubation at room temperature with gentle shaking, the reaction was stopped by adding equal volume of ADP-Glo buffer and incubated for another hour to remove excess amount of ATP from the reaction. Afterwards, 10  $\mu\text{L}$  of kinase detection reagent was added, mixed, and incubated for 30 min under dark. Luminescence output was recorded using a SpectraMax M5 Multi-Mode Microplate Readers (Molecular Devices, San Jose, CA), an integration time of 500 ms was used. All reactions were performed in triplicated. The enzyme activity of SphK in the presence of each compound was normalized to the no treatment control. To determine the  $\text{IC}_{50}$  of each compound on SphK2, series dilutions of each compound ranging from 1.25 mM to 1.25 pM were tested in the presence of 50  $\mu\text{M}$  of ATP. The final data was calculated using Prism 7.0 (GraphPad Software, La Jolla, CA),  $\text{IC}_{50}$  was determined using Nonlinear regression (curve fit) four parameters dose-response calculations.

#### 4.3.3. *Molecular modeling and molecular docking*

The homology model for SphK2 was developed using the I-TASSER server with the canonical sequence of SphK2 (UniProtKB: Q9NRA0-1). A total of 5 models were produced, and the second ranking model was selected (C-score = -2.36) following visual inspection and comparison with known structures of SphK1. The homology model was further refined using the protein preparation wizard in Maestro through side chain protonation (pH 5-9), h-bond optimization and a restrained minimization (heavy atoms converged to 0.3 Å) (Schrödinger Release 2018-4: Maestro, version 11.8, Schrödinger, LLC, New York, NY (2018) Schrödinger Suite 2018 Protein Preparation Wizard; Schrodinger, LLC, New York (2018). Three-dimensional representations and protonation state of compound **29a** were prepared using Ligprep (LigPrep, Schrodinger, LLC, New York (2015)). The induced fit docking

protocol was carried out with extended sampling, and the binding site was identified by aligning the SphK2 homology model with SphK1 (PDB: 4V24) [55]. The resulting ensemble of docking poses were clustered by protein interaction fingerprint and the top scoring poses from each cluster were selected for binding pose metadynamics [56]. Binding pose metadynamics (ten simulations of 10 ns) were carried out on an NVIDIA P100 GPU using default parameters as previously described [47]. The top-scoring pose (Pose Score = 1.2) was selected for further analysis.

#### 4.3.4. *In vitro cell viability assay*

U-251 MG cells were kindly given by Dr. Vaishali Kapoor (Department of Radiation Oncology, Washington University School of Medicine). In brief, cells were cultured in RPMI-1640 supplemented with 10% FBS, 1 mM Sodium Pyruvate, and 1x Pen-Strep (ThermoFisher, Waltham, MA) and maintained at 37 °C and 5% CO<sub>2</sub> incubator. Cells were seeded into a 96-well microplate (Corning, Corning, NY) at 3000 cells/well and incubated for approximately 16 hours. After that, medium was replaced with fresh medium containing 125 μM of each compound and incubated for 24 hours. Cell viability was determined by staining with Hoechst 33258 for total cells and propidium iodide for apoptotic cells (Biotium, Fremont, CA). Cells were imaged using MetaXpress High-Content Image Acquisition and Analysis Software 6.1 and ImageXpress Micro XLS Wide-field High-Content Analysis System (Molecular Devices, San Jose, CA). Images were taken with a Nikon 10X CFI Plan Fluor objective. For all samples, triplicated measurements were performed. All images were processed and analyzed automatically using batch processing in Fiji ImageJ [57].

#### **Declaration of competing interest**

The authors declare that they have no known competing financial interests or personal relationships that could have appeared to influence the work reported in this paper.

## Acknowledgements

This study was supported by the USA National Institutes of Health including the National Institute of Neurological Disorders and Stroke, the National Institute on Aging [NS075527 and NS103988], the Barnes Jewish Hospital Foundation, the American Parkinson Disease Association (APDA) and the Greater St. Louis Chapter of the APDA.

## Appendix A. Supplementary data

Supplementary data to this article can be found at online.

## References

- [1] H. Chi, Sphingosine-1-phosphate and immune regulation: trafficking and beyond, *Trends Pharmacol. Sci.* 32 (2011) 16-24.
- [2] N. Takasugi, T. Sasaki, K. Suzuki, S. Osawa, H. Isshiki, Y. Hori, N. Shimada, T. Higo, S. Yokoshima, T. Fukuyama, V.M. Lee, J.Q. Trojanowski, T. Tomita, T. Iwatsubo, BACE1 activity is modulated by cell-associated sphingosine-1-phosphate, *J. Neurosci.* 31 (2011) 6850-6857.
- [3] B. Prager, S.F. Spampinato, R.M. Ransohoff, Sphingosine 1-phosphate signaling at the blood-brain barrier, *Trends Mol. Med.* 21 (2015) 354-363.
- [4] L.A. Heffernan-Stroud, L.M. Obeid, Sphingosine kinase 1 in cancer, *Adv. Cancer Res.* 117 (2013) 201-235.
- [5] N.J. Pyne, F. Tonelli, K.G. Lim, J.S. Long, J. Edwards, S. Pyne, Sphingosine 1-phosphate signalling in cancer, *Biochem. Soc. Trans.* 40 (2012) 94-100.

- [6] D. Plano, S. Amin, A.K. Sharma, Importance of sphingosine kinase (SphK) as a target in developing cancer therapeutics and recent developments in the synthesis of novel SphK inhibitors, *J. Med. Chem.* 57 (2014) 5509-5524.
- [7] N.J. Pyne, S. Pyne, Sphingosine 1-phosphate and cancer, *Nat. Rev. Cancer* 10 (2010) 489-503.
- [8] S.P. Reid, S.R. Tritsch, K. Kota, C.Y. Chiang, L. Dong, T. Kenny, E.E. Brueggemann, M.D. Ward, L.H. Cazares, S. Bavari, Sphingosine kinase 2 is a chikungunya virus host factor co-localized with the viral replication complex, *Emerg. Microbes Infect.* 4 (2015) e61.
- [9] S. An, Y. Zheng, T. Bleu, Sphingosine 1-phosphate-induced cell proliferation, survival, and related signaling events mediated by G protein-coupled receptors Edg3 and Edg5, *J. Biol. Chem.* 275 (2000) 288-296.
- [10] A. Olivera, T. Kohama, L. Edsall, V. Nava, O. Cuvillier, S. Poulton, S. Spiegel, Sphingosine Kinase Expression Increases Intracellular Sphingosine-1-Phosphate and Promotes Cell Growth and Survival, *J. Cell Biol.* 147 (1999) 545-558.
- [11] D.D. Song, J.H. Zhou, R. Sheng, Regulation and function of sphingosine kinase 2 in diseases, *Histol. Histopathol.*, 33 (2018) 433-445.
- [12] K. Quint, N. Stiel, D. Neureiter, H.U. Schlicker, C. Nimsky, M. Ocker, H. Strik, M.A. Kolodziej, The role of sphingosine kinase isoforms and receptors S1P1, S1P2, S1P3, and S1P5 in primary, secondary, and recurrent glioblastomas, *Tumour Biol.* 35 (2014) 8979-8989.
- [13] H. Liu, M. Sugiura, V.E. Nava, L.C. Edsall, K. Kono, S. Poulton, S. Milstien, T. Kohama, S. Spiegel, Molecular cloning and functional characterization of a novel mammalian sphingosine kinase type 2 isoform, *J. Biol. Chem.*, 275 (2000) 19513-19520.

- [14] H.A. Neubauer, S.M. Pitson, Roles, regulation and inhibitors of sphingosine kinase 2, *Febs j.* 280 (2013) 5317-5336.
- [15] G.T. Kunkel, M. Maceyka, S. Milstien, S. Spiegel, Targeting the sphingosine-1-phosphate axis in cancer, inflammation and beyond, *Nat. Rev. Drug Discov.* 12 (2013) 688-702.
- [16] M. Maceyka, K.B. Harikumar, S. Milstien, S. Spiegel, Sphingosine-1-phosphate signaling and its role in disease, *Trends Cell Biol.* 22 (2012) 50-60.
- [17] N.C. Hait, J. Allegood, M. Maceyka, G.M. Strub, K.B. Harikumar, S.K. Singh, C. Luo, R. Marmorstein, T. Kordula, S. Milstien, S. Spiegel, Regulation of histone acetylation in the nucleus by sphingosine-1-phosphate, *Science* 325 (2009) 1254-1257.
- [18] N. Igarashi, T. Okada, S. Hayashi, T. Fujita, S. Jahangeer, S. Nakamura, Sphingosine kinase 2 is a nuclear protein and inhibits DNA synthesis, *J. Biol. Chem.* 278 (2003) 46832-46839.
- [19] G. Ding, H. Sonoda, H. Yu, T. Kajimoto, S.K. Goparaju, S. Jahangeer, T. Okada, S. Nakamura, Protein kinase D-mediated phosphorylation and nuclear export of sphingosine kinase 2, *J. Biol. Chem.* 282 (2007) 27493-27502.
- [20] T. Okada, G. Ding, H. Sonoda, T. Kajimoto, Y. Haga, A. Khosrowbeygi, S. Gao, N. Miwa, S. Jahangeer, S. Nakamura, Involvement of N-terminal-extended form of sphingosine kinase 2 in serum-dependent regulation of cell proliferation and apoptosis, *J. Biol. Chem.* 280 (2005) 36318-36325.
- [21] H. Rosen, P.J. Gonzalez-Cabrera, M.G. Sanna, S. Brown, Sphingosine 1-phosphate receptor signaling, *Annu. Rev. Biochem.* 78 (2009) 743-768.

- [22] Y. Kharel, E.A. Morris, M.D. Congdon, S.B. Thorpe, J.L. Tomsig, W.L. Santos, K.R. Lynch, Sphingosine Kinase 2 Inhibition and Blood Sphingosine 1-Phosphate Levels, *J. Pharmacol. Exp. Ther.* 355 (2015) 23-31.
- [23] M.E. Schnute, M.D. McReynolds, T. Kasten, M. Yates, G. Jerome, J.W. Rains, T. Hall, J. Chrencik, M. Kraus, C.N. Cronin, M. Saabye, M.K. Highkin, R. Broadus, S. Ogawa, K. Cukyne, L.E. Zawadzke, V. Peterkin, K. Iyanar, J.A. Scholten, J. Wendling, H. Fujiwara, O. Nemirovskiy, A.J. Wittwer, M.M. Nagiec, Modulation of cellular S1P levels with a novel, potent and specific inhibitor of sphingosine kinase-1, *Biochem. J.* 444 (2012) 79-88.
- [24] D.J. Gustin, Y. Li, M.L. Brown, X. Min, M.J. Schmitt, M. Wanska, X. Wang, R. Connors, S. Johnstone, M. Cardozo, A.C. Cheng, S. Jeffries, B. Franks, S. Li, S. Shen, M. Wong, H. Wesche, G. Xu, T.J. Carlson, M. Plant, K. Morgenstern, K. Rex, J. Schmitt, A. Coxon, N. Walker, F. Kayser, Z. Wang, Structure guided design of a series of sphingosine kinase (SphK) inhibitors, *Bioorg. Med. Chem. Lett.* 23 (2013) 4608-4616.
- [25] N.N. Patwardhan, E.A. Morris, Y. Kharel, M.R. Raje, M. Gao, J.L. Tomsig, K.R. Lynch, W.L. Santos, Structure-activity relationship studies and in vivo activity of guanidine-based sphingosine kinase inhibitors: discovery of SphK1- and SphK2-selective inhibitors, *J. Med. Chem.* 58 (2015) 1879-1899.
- [26] M.R. Pitman, J.A. Powell, C. Coolen, P.A. Moretti, J.R. Zebol, D.H. Pham, J.W. Finnie, A.S. Don, L.M. Ebert, C.S. Bonder, B.L. Gliddon, S.M. Pitson, A selective ATP-competitive sphingosine kinase inhibitor demonstrates anti-cancer properties, *Oncotarget* 6 (2015) 7065-7083.
- [27] M.E. Schnute, M.D. McReynolds, J. Carroll, J. Chrencik, M.K. Highkin, K. Iyanar, G. Jerome, J.W. Rains, M. Saabye, J.A. Scholten, M. Yates, M.M. Nagiec, Discovery of a Potent and Selective Sphingosine Kinase 1 Inhibitor through the Molecular Combination of Chemotype-Distinct Screening Hits, *J. Med. Chem.* 60 (2017) 2562-2572.

- [28] K.J. French, Y. Zhuang, L.W. Maines, P. Gao, W. Wang, V. Beljanski, J.J. Upson, C.L. Green, S.N. Keller, C.D. Smith, Pharmacology and antitumor activity of ABC294640, a selective inhibitor of sphingosine kinase-2, *J. Pharmacol. Exp. Ther.* 333 (2010) 129-139.
- [29] K. Liu, T.L. Guo, N.C. Hait, J. Allegood, H.I. Parikh, W. Xu, G.E. Kellogg, S. Grant, S. Spiegel, S. Zhang, Biological characterization of 3-(2-amino-ethyl)-5-[3-(4-butoxyl-phenyl)-propylidene]-thiazolidine-2,4-dione (K145) as a selective sphingosine kinase-2 inhibitor and anticancer agent, *PLoS One* 8 (2013) e56471.
- [30] K.G. Lim, C. Sun, R. Bittman, N.J. Pyne, S. Pyne, (R)-FTY720 methyl ether is a specific sphingosine kinase 2 inhibitor: Effect on sphingosine kinase 2 expression in HEK 293 cells and actin rearrangement and survival of MCF-7 breast cancer cells, *Cell Signal* 23 (2011) 1590-1595.
- [31] J.W. Kim, Y.W. Kim, Y. Inagaki, Y.A. Hwang, S. Mitsutake, Y.W. Ryu, W.K. Lee, H.J. Ha, C.S. Park, Y. Igarashi, Synthesis and evaluation of sphingoid analogs as inhibitors of sphingosine kinases, *Bioorg. Med. Chem.* 13 (2005) 3475-3485.
- [32] M.R. Raje, K. Knott, Y. Kharel, P. Bissel, K.R. Lynch, W.L. Santos, Design, synthesis and biological activity of sphingosine kinase 2 selective inhibitors, *Bioorg. Med. Chem.* 20 (2012) 183-194.
- [33] E.S. Childress, Y. Kharel, A.M. Brown, D.R. Bevan, K.R. Lynch, W.L. Santos, Transforming sphingosine kinase 1 inhibitors into dual and sphingosine kinase 2 selective inhibitors: design, synthesis, and in vivo activity, *J. Med. Chem.* 60 (2017) 3933-3957.
- [34] C.D. Sibley, E.A. Morris, Y. Kharel, A.M. Brown, T. Huang, D.R. Bevan, K.R. Lynch, W.L. Santos, Discovery of a small side cavity in sphingosine kinase 2 that enhances inhibitor potency and selectivity, *J. Med. Chem.* 63 (2020) 1178-1198.

- [35] V.V. Rostovtsev, L.G. Green, V.V. Fokin, K.B. Sharpless, A stepwise Huisgen cycloaddition process: copper(I)-catalyzed regioselective "ligation" of azides and terminal alkynes, *Angew. Chem. Int. Ed. Engl.* 41 (2002) 2596-2599.
- [36] T. Vijai Kumar Reddy, A. Jyotsna, B.L. Prabhavathi Devi, R.B. Prasad, Y. Poornachandra, C. Ganesh Kumar, Design, synthesis and in vitro biological evaluation of short-chain C12-sphinganine and its 1,2,3-triazole analogs as potential antimicrobial and anti-biofilm agents, *Eur. J. Med. Chem.* 118 (2016) 98-106.
- [37] F.C. Schaefer, G.A. Peters, Base-Catalyzed Reaction of Nitriles with Alcohols. A convenient route to imidates and amidine salts, *J. Org. Chem.* 26 (1961) 412-418.
- [38] B.M. Buehrer, R.M. Bell, Inhibition of sphingosine kinase in vitro and in platelets. Implications for signal transduction pathways, *J. Biol. Chem.* 267 (1992) 3154-3159.
- [39] T.A. Klink, K.M. Kleman-Leyer, A. Kopp, T.A. Westermeyer, R.G. Lowery, Evaluating PI3 kinase isoforms using Transcreeper ADP assays, *J. Biomol. Screen.* 13 (2008) 476-485.
- [40] P.R. Patel, H. Sun, S.Q. Li, M. Shen, J. Khan, C.J. Thomas, M.I. Davis, Identification of potent Yes1 kinase inhibitors using a library screening approach, *Bioorg. Med. Chem. Lett.* 23 (2013) 4398-4403.
- [41] R. Nagaraj, M.S. Sharpley, F. Chi, D. Braas, Y. Zhou, R. Kim, A.T. Clark, U. Banerjee, Nuclear localization of mitochondrial TCA cycle enzymes as a critical step in mammalian zygotic genome activation, *Cell* 168 (2017) 210-223.e211.
- [42] C.D. Parks, Z. Gaieb, M. Chiu, H. Yang, C. Shao, W.P. Walters, J.M. Jansen, G. McGaughey, R.A. Lewis, S.D. Bembenek, M.K. Ameriks, T. Mirzadegan, S.K. Burley, R.E. Amaro, M.K. Gilson, D3R

grand challenge 4: blind prediction of protein–ligand poses, affinity rankings, and relative binding free energies, *J. Comput. Aided Mol. Des.* 34 (2020) 99-119.

[43] T.I. Croll, M.D. Sammito, A. Kryshchuk, R.J. Read, Evaluation of template-based modeling in CASP13, *Proteins: Structure, Function, and Bioinformatics*, 87 (2019) 1113-1127.

[44] J. Yang, R. Yan, A. Roy, D. Xu, J. Poisson, Y. Zhang, The I-TASSER Suite: protein structure and function prediction, *Nat.Methods* 12 (2015) 7-8.

[45] A. Roy, A. Kucukural, Y. Zhang, I-TASSER: a unified platform for automated protein structure and function prediction, *Nat. Protoc.* 5 (2010) 725-738.

[46] Y. Zhang, I-TASSER server for protein 3D structure prediction, *BMC Bioinformatics* 9 (2008) 40.

[47] A.J. Clark, P. Tiwary, K. Borrelli, S. Feng, E.B. Miller, R. Abel, R.A. Friesner, B.J. Berne, Prediction of protein–ligand binding poses via a combination of induced fit docking and metadynamics simulations, *J. Chem. Theory Comput.*, 12 (2016) 2990-2998.

[48] M. Aldeghi, A. Heifetz, M.J. Bodkin, S. Knapp, P.C. Biggin, Accurate calculation of the absolute free energy of binding for drug molecules, *Chem. Sci.* 7 (2016) 207-218.

[49] J.R. Van Brocklyn, C.A. Jackson, D.K. Pearl, M.S. Kotur, P.J. Snyder, T.W. Prior, Sphingosine kinase-1 expression correlates with poor survival of patients with glioblastoma multiforme: roles of sphingosine kinase isoforms in growth of glioblastoma cell lines, *J. Neuropathol. Exp. Neurol.* 64 (2005) 695-705.

[50] P.L. Kornblith, M. Walker, Chemotherapy for malignant gliomas, *J. Neurosurg.* 68 (1988) 1-17.

[51] L.A. Sordillo, P.P. Sordillo, L. Helson, Sphingosine kinase inhibitors as maintenance therapy of glioblastoma after ceramide-induced response, *Anticancer Res.* 36 (2016) 2085-2095.

- [52] V. Beljanski, C. Knaak, C.D. Smith, A novel sphingosine kinase inhibitor induces autophagy in tumor cells, *J. Pharmacol. Exp. Ther.* 333 (2010) 454-464.
- [53] J.W. Antoon, M.D. White, E.M. Slaughter, J.L. Driver, H.S. Khalili, S. Elliott, C.D. Smith, M.E. Burow, B.S. Beckman, Targeting NF $\kappa$ B mediated breast cancer chemoresistance through selective inhibition of sphingosine kinase-2, *Cancer Biol. Ther.* 11 (2011) 678-689.
- [54] F. Sievers, A. Wilm, D. Dineen, T.J. Gibson, K. Karplus, W. Li, R. Lopez, H. McWilliam, M. Remmert, J. Söding, J.D. Thompson, D.G. Higgins, Fast, scalable generation of high-quality protein multiple sequence alignments using Clustal Omega, *Mol. Syst. Biol.* 7 (2011) 539.
- [55] W. Sherman, T. Day, M.P. Jacobson, R.A. Friesner, R. Farid, Novel procedure for modeling ligand/receptor induced fit effects, *J. Med. Chem.* 49 (2006) 534-553.
- [56] Z. Deng, C. Chuaqui, J. Singh, Structural Interaction Fingerprint (SIFt): A Novel method for analyzing three-dimensional protein–ligand binding interactions, *J. Med. Chem.* 47 (2004) 337-344.
- [57] J. Schindelin, I. Arganda-Carreras, E. Frise, V. Kaynig, M. Longair, T. Pietzsch, S. Preibisch, C. Rueden, S. Saalfeld, B. Schmid, J.Y. Tinevez, D.J. White, V. Hartenstein, K. Eliceiri, P. Tomancak, A. Cardona, Fiji: an open-source platform for biological-image analysis, *Nat. Methods* 9 (2012) 676-682.

## Highlights

- Eighteen 1,2,3-triazole containing new selective SphK2 inhibitors were synthesized
- All synthesized compounds were screened for their *in vitro* biological activities using ADP-Glo kinase assay
- Most of the synthesized compounds showed high specificity to SphK2 over SphK1
- Compound **21g** displayed the most potent *in vitro* SphK2 inhibition ( $IC_{50} = 0.23 \mu M$ )
- Discovered three compounds having potential anti-glioblastoma multiform activity

**Declaration of interests**

The authors declare that they have no known competing financial interests or personal relationships that could have appeared to influence the work reported in this paper.

The authors declare the following financial interests/personal relationships which may be considered as potential competing interests:

Journal Pre-proof